Geomorphology 503 (2026) 110297

Contents lists available at ScienceDirect

Geomorphology

journal homepage: www.journals.elsevier.com/geomorphology

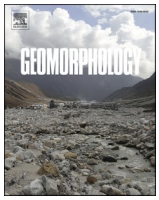

Assessing potential controls on river bead functionality in mountain streams

Katie Larkin *, Ellen Wohl

Department of Geosciences, Colorado State University, Fort Collins, CO, 80523-1482, USA

ARTICLE INFO

Keywords:
Flux attenuation
Spatial heterogeneity
Storage
Floodplain-channel connectivity
River restoration
Beaver
Logjams
Riparian vegetation

ABSTRACT

Storage-dominated alluvial reaches of river corridor in mountain streams, known as river beads, provide disproportionately important attenuation of downstream fluxes of diverse materials at local- to network-scales. We refer to attenuation as bead functionality. We evaluated potential controls on functionality in beads by statistically evaluating relationships between 28 driver and 5 response variables. Driver variables represent inputs of water and sediment and biophysical interactions that could influence bead functionality. Geomorphic driver variables represent water inputs to the stream corridor (e.g., drainage area, catchment slope, elevation, land cover, precipitation metrics), sediment inputs (catchment slope, the metric of normalized burn index), and bead geometry (e.g., bead size, floodplain/channel width ratio). Biotic driver variables within each bead include wood load, beaver modifications, and type of riparian vegetation. Response variables are proxies for attenuation and storage within river beads. Response variables include greenness (normalized difference vegetation index), wetness (normalized difference water index), patch density, patch count, and total sinuosity. Driver and response variables were measured through a mixture of fieldwork and remote data for 52 beads in 27 catchments in the Colorado Front Range, USA. Statistical analyses examined relationships between drivers and responses and the effectiveness of grouping the beads by dominant vegetation and by elevation zone. Analyses suggest that bead functionality is most strongly linked to bead ratio, or the ratio of bead size to catchment size. Functional beads are larger relative to catchment size. In addition, bead types grouped by dominant vegetation reflect significant differences in catchment geometry, geomorphic inputs, and biotic inputs, and display significant differences in bead geometry. Although functionality is the complex result of numerous factors and may require case-by-case assessment efforts, restoration of channel-floodplain connectivity and facilitating greater retention of water will enhance bead functionality by increasing the width of the active floodplain. Investigating drivers of functionality provides a crucial link between system inputs, restoration action, and desired response, allowing plans to be tailored to address targets. Because bead position and geometry cannot be feasibly modified, the functionality framework can be used to identify sites with the greatest potential for restoration.

1. Introduction

Describing hyporheic exchanges in gravel-bed river corridors, Stanford and Ward (1993) noted that alluvial reaches occur serially, like beads on a string, between more laterally confined, bedrock-bounded lengths of river corridor. The description of alternating laterally confined and relatively unconfined reaches as river beads and strings provides a simple descriptive phrase for a commonly occurring pattern in rivers flowing through moderate- to high-relief terrain (Fig. 1). The longitudinal alternation between river beads and strings can result from longitudinal variation in glacial history or bedrock lithology or structure (Ehlen and Wohl, 2002) and can affect river corridors from the headwaters to major rivers.

River beads have greater space for floodplain formation, lateral channel movements, and the erosion and deposition associated with channel movements and with channel-floodplain connectivity. Consequently, river beads commonly have greater spatial and temporal heterogeneity than strings (e.g., Wyzga and Zawiejska, 2005; Marshall et al., 2024). We describe spatial heterogeneity as topographic variations in the channel and floodplain, as well as the associated variations in sediment grain-size distribution, soil moisture, hyporheic and groundwater movements, and vegetation communities (Wohl, 2016;

* Corresponding author.
E-mail address: katie.larkin@colostate.edu (K. Larkin).

https://doi.org/10.1016/j.geomorph.2026.110297
Received 10 September 2025; Received in revised form 18 March 2026; Accepted 20 March 2026
Available online 21 March 2026

Iskin and Wohl, 2023).

Differences in spatial and temporal heterogeneity between river beads and strings equate to substantial differences in processes and functions (Bellmore and Baxter, 2014; Hauer et al., 2016; Wohl et al., 2018, 2025a, 2025b). River strings provide relatively efficient downstream conveyance for materials, including water, solutes, sediment, particulate organic matter, and large wood. These transport-dominated reaches provide longitudinal connectivity within the river network but are relatively ineffective at attenuating downstream fluxes.

River beads, in contrast, typically have greater accommodation space for surface and subsurface storage of materials and are more effective at attenuating downstream fluxes. Attenuation here refers to a decrease in peak discharge of materials moving downstream by prolonging the travel time of materials. Spatial heterogeneity and attenuation can be correlated because greater spatial heterogeneity increases hydraulic resistance, areas of flow separation, and diversity of transport pathways, thus increasing attenuation (Lininger and Latrubesse, 2016; Christensen and Morrison, 2026).

Attenuation of peak and base flows can occur through storage in no- or low-velocity areas such as the floodplain or subsurface for varying lengths of time and through travel paths of differing lengths and speeds, such as secondary channels (Wohl et al., 2025a, 2025b; Christensen and Morrison, 2026). Beads are likely to have greater hyporheic and groundwater exchanges (Schulz et al., 2024; Gambill et al., 2025) and more diverse flow paths and hydrologic residence times (Helton et al., 2014) than strings.

Beads and their floodplains can also effectively attenuate downstream fluxes of sediment by storing sediment in channel bars and the floodplain (Walling and He, 1998; Fryirs et al., 2007; Wohl, 2021a). Greater spatial heterogeneity of beads corresponds to greater habitat diversity, which can help to foster biomass and biodiversity (Bellmore and Baxter, 2014; Spurgeon et al., 2018; Stoffers et al., 2022); greater trophic complexity or food chain length in river ecosystems (Thoms et al., 2017); increased nutrient uptake (Appling et al., 2014); and increased storage of organic carbon (Wohl et al., 2012, 2018; Langhans et al., 2013; Sutfin et al., 2021).

River functionality can be described in the context of multiple processes and forms, including ecological functions such as decomposition and sediment respiration (Feio et al., 2010), habitat diversity (Kemp et al., 1999), and user-functions such as navigation and flood protection (Hiemstra et al., 2020). Here, we describe river bead functionality as the ability to attenuate downstream fluxes of diverse materials and we assume that greater spatial heterogeneity equates to increased functionality.

By attenuating fluxes and providing habitat and refugia for diverse riverine organisms, river beads can increase resilience to disturbance at reach- and network-scales (Wohl et al., 2018, 2025a, 2025b; Morrison et al., 2024). Resilience here refers to the ability to sustain or rapidly recover riverine functionality following disturbances such as wildfire, drought, or flood. River beads are likely to be disproportionately important, relative to the total proportion of river corridor length that they occupy in a network, in sustaining resilience (Biron et al., 2014; Wohl et al., 2018, 2022, 2024a; Van Looy et al., 2019; Hahn et al., 2025).

Beads can promote attenuation of downstream fluxes if the channel and floodplain are connected and if the river corridor possesses the physical integrity (Graf, 2001) that permits continued erosion and deposition that maintain heterogeneity. However, diverse human alterations including channel incision, artificial levees, bank stabilization, and flow regulation can effectively disconnect the channel from the floodplain within a river bead. Disconnection of the floodplain and channel equates to loss of physical integrity and loss of spatial and temporal heterogeneity in river corridors (Moyle and Mount, 2007; Peipoch et al., 2015; DeBoer et al., 2020). As heterogeneity declines, river beads are likely to create less attenuation although even a relatively homogeneous floodplain still provides some storage space and attenuation if it remains connected to the channel.

Given widespread loss of spatial and temporal heterogeneity in river corridors (Peipoch et al., 2015) and changing disturbance regimes that highlight the need for increased resilience in river corridors (Thoms and Fuller, 2023), river beads are increasingly the focus of management and restoration designed to increase resilience to disturbances (e.g., Serra-Llobet et al., 2022). In the United Kingdom, natural flood management emphasizes the use of leaky dams, off- and on-channel storage ponds, and beaver reintroduction to reduce flood peaks (Lane, 2017; Wilkinson et al., 2019; Puttock et al., 2021). In the western United States, where increasing frequency, extent, and severity of wildfires are stressing human and biotic communities (Westerling, 2016), river restoration commonly focuses on increasing the heterogeneity of river beads via (i) valley reset or Stage 0 methods that seek to reconfigure the river corridor and introduce obstacles in the active channel to hydrologically and geomorphically reconnect the channel and floodplain (Powers et al., 2019; Flitcroft et al., 2022; Clarke, 2025), (ii) reintroduction of beaver or mimicry of beaver dams (Bouwes et al., 2016; Pearce et al., 2021;

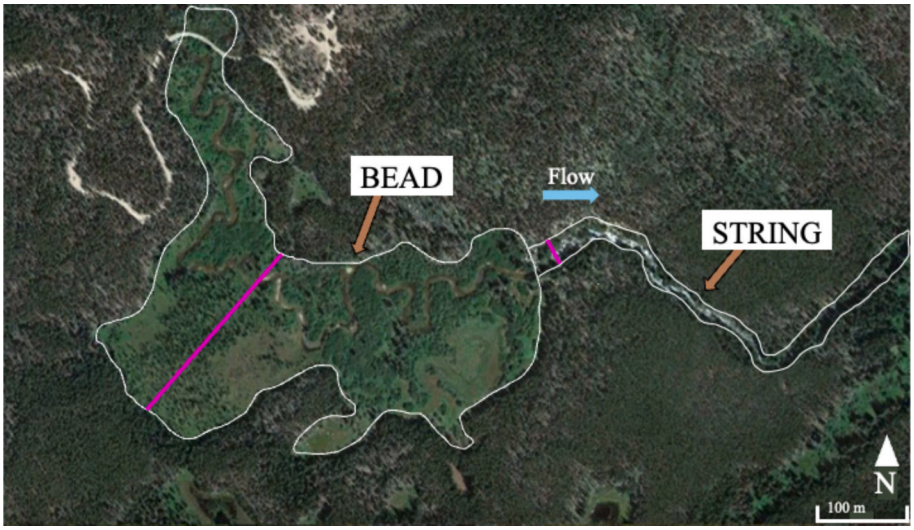

Fig. 1. Aerial comparison of a bead and string on Beaver Creek, Colorado. Maximum river corridor width (shown as a red line) is ~223 m in the bead and ~ 34 m in the string. Imagery provided by Google Earth Pro (Landsat/Copernicus, 2025). (For interpretation of the references to colour in this figure legend, the reader is referred to the web version of this article.)

Meyer et al., 2025), and (iii) reintroduction of large wood (Pugh et al., 2022; Ockelford et al., 2024), all with the intent of attenuating flood peaks and sediment yields during post-fire storms and restoring other impaired river functions such as biodiversity.

1.1. Conceptual model of bead functionality

We developed a conceptual model of the influences on bead functionality for river beads in the Colorado Front Range, which typically has forested river corridors and uplands and valley-floor modifications by North American beaver (*Castor canadensis*). We assume that the location and basic geometry (width, downstream gradient) of each river bead reflect the underlying geologic template. Inputs of water, sediment, and large wood from adjacent uplands and upstream portions of the river network then interact with this template and with vegetation and beaver modifications (dams, ponds, canals) in the river corridor to create spatial heterogeneity, three-dimensional connectivity, and resultant attenuation of material fluxes and resilience to disturbance. Greater heterogeneity, lateral and vertical connectivity, attenuation of fluxes, and resilience equate to greater bead functionality. Fig. 2 illustrates these relationships and lists the proxy variables that we assessed for inputs, river bead geometry, biotic influences, and functionality. These proxy variables are explained in Methods.

1.2. Objectives and hypotheses

We examined river beads in the U.S. Southern Rocky Mountains with the objectives of assessing (i) bead functionality using proxy variables and (ii) correlations between potential driver variables and functionality proxy variables. The proxy variables for bead functionality are greenness (represented by normalized difference vegetation index, NDVI), wetness (normalized difference water index, NDWI), patch density, patch count, and total channel sinuosity. The potential driver variables include a long list of catchment characteristics that might influence water, sediment, and large wood inputs to each bead, as well as descriptors of bead geometry that influence the ability to develop spatial heterogeneity through processes such as channel movement, large wood deposition, and beaver modifications.

We selected beads across two elevation zones (subalpine, montane) in the study area. Elevation zones in the study area correspond to differences in riparian and upland vegetation, disturbance regime, and flow regime that could influence bead functionality, as explained in the Study Area. We also designated each bead as one of three types (beaver meadow, elk grassland, forested river corridor), differentiated primarily on the dominant class and spatial extent of floodplain vegetation. Beaver meadow, elk grassland, and forested beads are dominated by willow carrs, grasses, and conifers, respectively, as explained in Methods. Vegetation type and extent in the floodplain and riparian zones can strongly influence hydraulic roughness and erosional resistance of stream banks and floodplain, modifying flux attenuation within beads (Barinas et al., 2024). Vegetation can also be indicative of floodplain-channel connectivity.

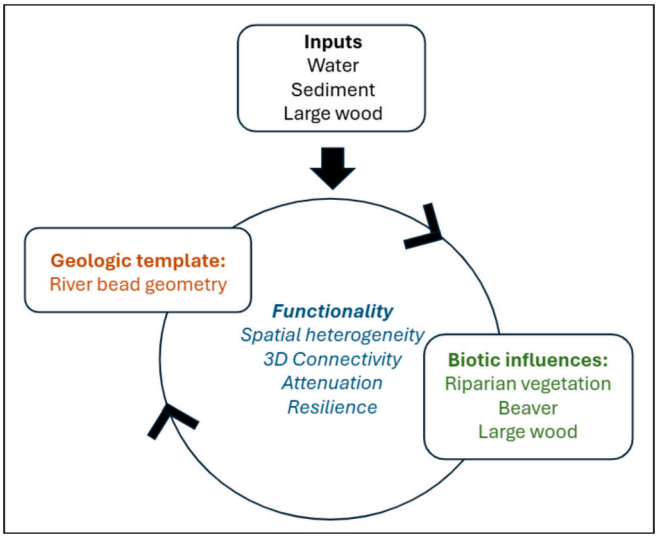

Fig. 2. Conceptual diagram of relationships among inputs, influences on bead characteristics, and bead functionality.

We differentiated bead types based on existing knowledge of the effects of riparian vegetation and beaver valley floor modifications on attenuation of water, sediment, and solutes moving downstream. Beaver modifications enhance floodplain-channel connectivity by slowing water velocity (Gurnell, 1998; Butler and Malanson, 2005; Green and Westbrook, 2009), trapping fine sediment (Polvi and Wohl, 2012; Dunn et al., 2024), promoting infiltration into the channel banks and from overbank flows (Larsen et al., 2021; Wohl, 2021b), and raising surface and subsurface water levels (Westbrook et al., 2006; Dittbrenner et al., 2022). Beaver-modified landscapes are also associated with higher vegetation species richness and increased landscape patchiness (Wright et al., 2002) as well as fire-resistant riparian buffers (Fairfax and Whittle, 2020).

Elk grasslands are relict beaver meadows altered after beaver abandon a stream corridor. Former beaver meadows may undergo incision following beaver disappearance from the site and evolve into a disconnected alternate system with single-thread channelization (Green and Westbrook, 2009; Polvi and Wohl, 2013), unstable banks, lowered water tables (Schumm et al., 1984), and decreased proportions of hydric vegetation (Miller et al., 2011), known as an elk grassland (Wolf et al., 2007; Beschta and Ripple, 2009). Elk grasslands and beaver meadows are considered end-member conditions representative of, respectively, high and low degrees of human, ungulate, and disturbance-related modifications impacting connectivity, heterogeneity, and flux attenuation potential in the channel and floodplain. Some elk grasslands retain signatures of beaver modification or geomorphic complexity, despite decreases in connectivity, and likewise some inactive beaver meadows show signs of connectivity loss; the meadow-grassland relationship is thus considered a continuum rather than a binary (Fig. 3).

We used characterization of these beads to test three hypotheses.

H1. River bead functionality will correlate strongly with bead type and elevation zone. The rationale underlying this hypothesis is that individual bead types represent different vegetation and spatial heterogeneity, which could influence hydraulic roughness, spatial heterogeneity, and attenuation of downstream fluxes. Each elevation zone represents a different flow and disturbance regime, which could also influence spatial heterogeneity and attenuation.

H2. River bead functionality correlates more strongly with multiple potential driver variables than with any single variable. The rationale underlying this hypothesis is that statistical analyses will reflect the interaction of multiple variables that influence river functionality.

H3. There is a progressive relationship between bead functionality and bead size. Bead size is characterized as bead surface area and the ratio of floodplain width to bankfull channel width. The rationale underlying this hypothesis is that as the lateral and longitudinal area of each bead increases, there is greater physical space for the development of spatial heterogeneity through erosion and deposition and the modifications created by beaver, which will increase attenuation of downstream fluxes.

2. Study area

We focus on the Colorado Front Range, a portion of the U.S. Southern Rocky Mountains, because of proximity to and prior work in the study

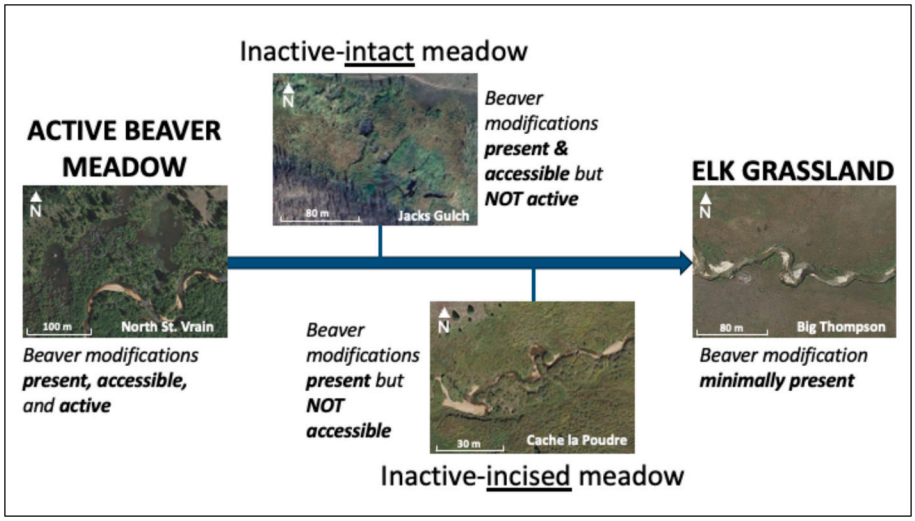

Fig. 3. Beaver meadow-elk grassland continuum as observed at four different field sites; accessible refers to beaver modifications interacting with the contemporary hydrologic regime of the stream. Imagery provided by Google Earth Pro (Landsat/Copernicus, 2025).

area, including knowledge of the attenuation function and disturbance history of river beads (e.g., Wohl et al., 2022), as well as the diversity of river beads with respect to size, type, elevation zone, and recent disturbance history including wildfires. The 2020 Cameron Peak wildfire, the largest in Colorado history at the time of writing, burnt approximately 88,634 ha (Swayze et al., 2021) from August 13 until December 2, 2020. An estimated 60% of the forested uplands of the Cache la Poudre River catchment (Thurman et al., 2023) burned, and 40% of the total burn area was classified as moderate- to high-severity (USDA Forest Service, 2020). The post-wildfire cascade in this region has been linked to poor downstream water quality, a severe debris flow, fish kill, and increased rates of sedimentation (Kean et al., 2022; Kostelnik et al., 2022). Many of the sub-catchments that we investigated were at least partly burned during the Cameron Peak fire and the post-fire disturbance cascade of increased water and sediment inputs to river corridors motivated our investigation.

Study catchments in the Colorado Front Range are underlain by Pre-Cambrian felsic crystalline igneous and metamorphic units (Tweto, 1979). Retreat of the last stage of Pleistocene glaciation began ~16,800 years ago (Madole, 1976; Benson et al., 2005), leaving expansive and flat river beads with sinuous channels and few bedrock constrictions (Livers and Wohl, 2015) and terminal moraines that facilitate deposition in beads. Several beads in this study within Rocky Mountain National Park are situated above the Pleistocene glacial terminal moraine (~2,430 m) deposited during the Pinedale glaciation (Wohl et al., 2004), and the headwaters of all three of the primary study catchments were glaciated during this period.

Mean annual precipitation is 70–80 cm in the upper elevations of the study area (Livers and Wohl, 2016), and streams have a snowmelt-dominated hydrograph that peaks during May–June. Mean annual precipitation in the lower elevations is ~36 cm. The Colorado Front Range is zoned by elevation into alpine (> 3,500 m elevation), subalpine (3,500–2,850 m), montane (2,850–1,750 m), and semi-arid steppe (< 1,550 m) ecoregions (Veblen and Donnegan, 2006). Study catchments are located in the subalpine and montane. Subalpine forests are dominated by Engelmann spruce (*Picea engelmannii*), subalpine fir (*Abies lasiocarpa),* aspen (*Populus tremuloides*), and lodgepole pine (*Pinus contorta*) (Chapman et al., 2006). Montane forests are dominated by aspen (*Populus tremuloides*), ponderosa pine (*Pinus ponderosa*), Douglas-fir (*Pseudotsuga menziesii*), lodgepole pine (*Pinus contorta*), and limber pine (*Pinus flexilis*) (Chapman et al., 2006). In both zones, understory and bead vegetation species vary with elevation, soil moisture, sun exposure, and disturbance history.

The annual flow regime is dominated by late spring-early summer snowmelt, with superimposed convective storms later in the summer. The nature and extent of snowpack varies year-to-year but is generally decreasing with warming climate (Pederson et al., 2013; Zanewich and Rood, 2025). Earlier arrivals of warmer temperatures alter hydrograph morphology to a constrained high-magnitude peak earlier in the spring and reduced peak flow in late spring and early summer (Rood et al., 2008).

The Cache la Poudre River, Big Thompson River, and North St. Vrain Creek catchments, all tributaries of the South Platte River, contain the sub-catchments investigated here (Fig. 4). A total of 52 beads in 27 different sub-catchments were identified, delineated, and evaluated for biotic and geomorphic functionality drivers (input variables), and functionality indicators (response variables). Bead size ranged from 1,330 m^2 to 452,000 m^2 and catchment size ranged from 363,000 m^2 to 234 km^2.

3. Methods

We defined a bead as a length of stream corridor in which average width of the active floodplain equaled or exceeded twice the average width of the active channel. The ratio of floodplain or flood-prone width to bankfull channel width is included in other studies as confinement index or entrenchment ratio (e.g., Kellerhals and Church, 1989; Polvi et al., 2011; Fryirs et al., 2016).

Drivers and functionality responses were measured in the field and remotely and assessed statistically. Field and remote analyses were undertaken simultaneously during summer and autumn 2024. Five beads in the dataset (Cony Creek, Hunters Creek, North St Vrain 1, North St Vrain 2, and Ouzel Creek) were fully characterized using the dataset of Bridget Livers (Livers and Wohl, 2016) and were not visited as part of this investigation. Of the 47 beads visited in the field, seven were not surveyed in their entirety due to length; longitudinal consistency of conditions was confirmed in the field, and a representative subset of the bead was surveyed instead.

Supplemental Table 1 lists and explains all variables and notes the method of data collection and whether the variable was used in statistical analyses. (From here on, we refer to variables and metrics as variables in the context of statistical analyses.) We started with 5 variables to characterize catchment geometry, 8 variables for bead geometry, 6 variables for biotic drivers (large wood, beaver modifications, riparian vegetation), 5 variables for hydrologic drivers, 3 for sediment drivers, and 5 response variables. Many of the variables were not retained during

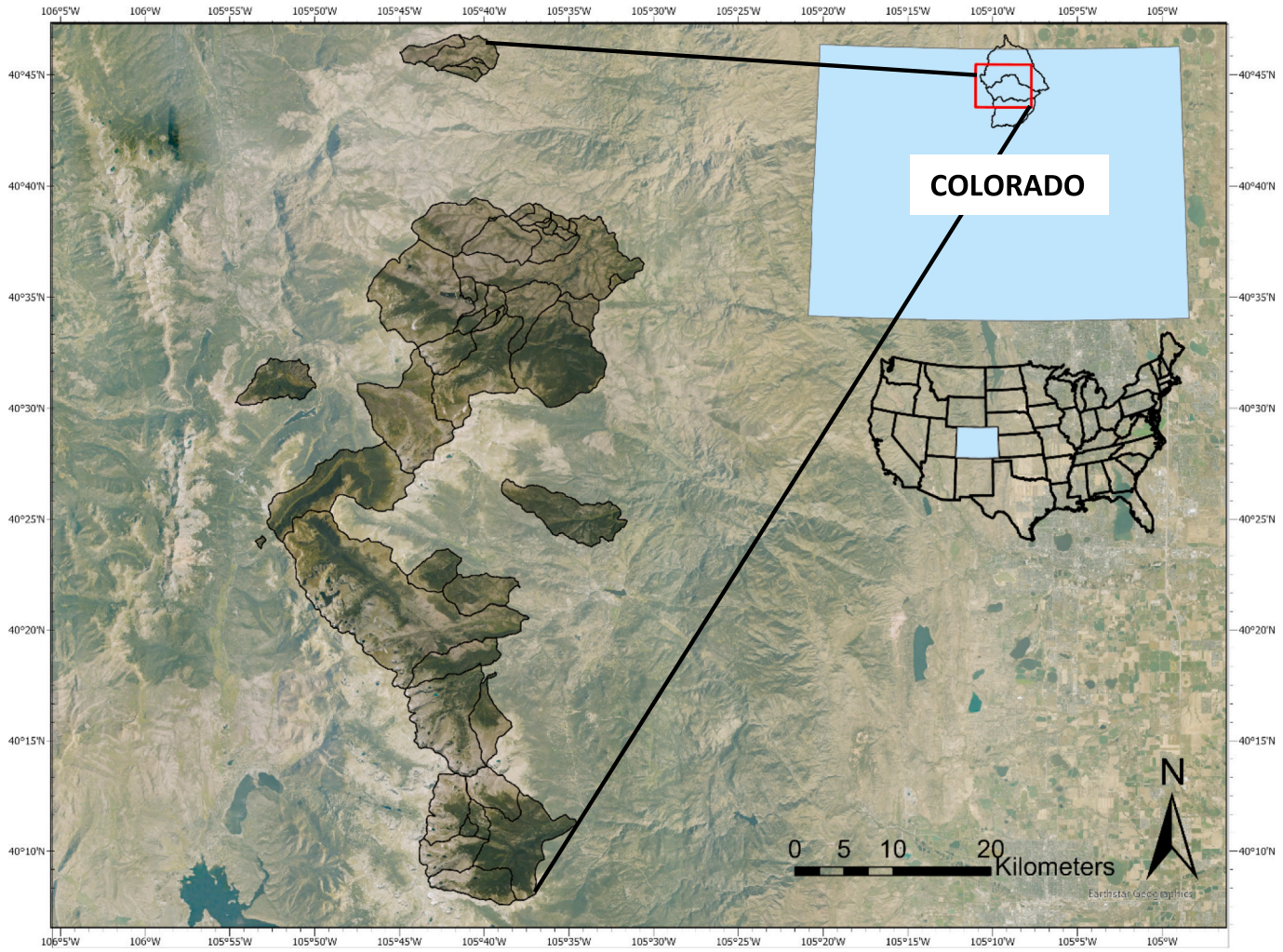

Fig. 4. Study subcatchments. Some catchments contain multiple studied beads. See Supplemental Table S3 for bead and subcatchment location specifics. The map was created with ESRI ArcGIS Pro Version 3.3.1 (2024) using catchment boundaries estimated by StreamStats.

statistical analyses either because of lack of significance or collinearity. Table 1 lists the variables retained for analyses.

3.1. Field-based data collection

Fieldwork verified bead geometry that was also assessed remotely, and also documented vegetation, measured wood volume, and assessed beaver modifications where present. Active channel width and flow depth were measured with a Laser Technology TruPulse 360 laser rangefinder (± 0.1 m resolution) and a hand tape, respectively, and bed substrate was assessed visually. Bead starting points ("inlets") and ending points ("outlets") were collected as points with a Garmin eTrex10 GNSS (Global Navigation Satellite System) receiver (± 3 m horizontal accuracy).

Vegetation, specifically dominant class and estimated spatial extent, was characterized visually in the field and used to classify beads (Fig. 5). Small conifer patches were observed in beaver meadows where soil was drier and/or topography was higher, but most vegetation in these beads is hydrophytic and includes willow (*Salix* spp.), herbaceous plants, and rushes or sedges. Conifer patches were more frequently observed in elk grasslands, but these beads generally supported higher proportions of grasses and relict willow stands. Vegetation heights in beaver meadow and elk grassland beads were generally <2 m.

In-channel deposits of woody material, including wood pieces and logjams, can reduce local water velocity (e.g., Shields and Smith, 1992; Daniels and Rhoads, 2003) and facilitate localized deposition and scour (Gurnell et al., 2002; Manners et al., 2007; Wohl and Scott, 2017). Wood pieces and accumulations are subject to changing distributions and orientations with respect to flow (Supplemental Fig. S1) as high flows alter their configurations and the ways they interact with the channel (Wohl and Iskin, 2022; Pavlowsky et al., 2023; Hortobagyi et al., 2024). Large wood (LW), defined as length ≥ 1 m and diameter ≥ 10 cm (Wohl et al., 2010) and logjams, defined as a cluster of three or more pieces of large wood (Wohl and Iskin, 2022), were documented in the field. Logjams and wood pieces were assigned a GPS location, width and length, diameter, and azimuthal direction, and characterized for their decay level, configuration, and complexity level. For larger jams, field-measured length, width, and height and an empirically derived estimated jam porosity of 0.5 were used to estimate total wood volume (Livers et al., 2020). Floodplain wood pieces, as well as wood of smaller lengths and/or widths, were not included in this study. All wood surveyed was at least partly within the bankfull channel.

GNSS locations and valley-bottom extent of both active and relict beaver berms were mapped in the field for each bead (Supplemental Figs. S2 and S3). Most berms at the study sites were relict. Field berm counts represent a minimum value; differences in topographic prominence, width, and length of berms abandoned for years to decades increase human error in their detection. Minimum berm count and primary channel length were used to calculate berm density, or the number of berms per kilometer of valley length. Nearly all berms were

Table 1
Variables used in statistical analyses.

Variable	Definition
Catchment Geometry	
Contributing drainage area (km^2)	Size of total contributing area to bead
Average catchment slope	Average slope over entire catchment
Average catchment elevation (m)	Average elevation over entire catchment
Mixed forest (%)	Percent of drainage area covered with National Land Cover Database (NLCD) 2021 classes 41–43 (Deciduous, Evergreen, and Mixed Forest)
Bead Geometry and Characteristics	
Bead Size (km^2)	Total area of flat, wide, floodplain associated with bead
Bead Slope	Valley slope from inlet to outlet of bead
Floodplain-channel ratio	Ratio of channel width to floodplain width
Bead ratio	Bead size divided by size of contributing drainage area
Biotic Drivers	
Wood Density	Approximate number of large wood pieces per kilometer
Minimum Berm Count	Total number of observed beaver berms in each bead
Berm Density (berms/km)	Approximate number of berms per unit channel length
Riparian buffer	Dominant vegetation and conditions
Geomorphic Drivers (Water)	
I6H100Y (mm)	6-h precipitation that is expected to occur on average once in 100 years
STORNHD (%)	Percent storage (wetlands and waterbodies) determined from 1:24 K National Hydrography Dataset (NHD)
1% Annual Exceedance Probability (AEP) (cms)	Maximum instantaneous flow that occurs with a 1% annual exceedance probability
50% AEP (cms)	Maximum instantaneous flow that occurs with a 50% annual exceedance probability
Precipitation (mm)	Mean annual precipitation
Geomorphic Drivers (Sediment)	
High Severity Burn (%)	Percent coverage of high severity burn in each catchment
Total Burn (%)	Percent coverage of burn of any severity in each catchment
Burn Ratio	Ratio of high severity catchment burn to total burn
Response Variables	
Total sinuosity	Sum of primary and secondary channel length, divided by valley length
Bead Normalized Difference Water Index (NDWI)	Remotely sensed indicator of water content and soil moisture
Bead Normalized Difference Vegetation Index (NDVI)	Remotely sensed indicator of vegetation health and stress
Patch count	Total number of observed patches in each bead
Patch density (patches/ km^2)	Approximate number of patches per unit area

valley-spanning, and total channel length was not used to calculate berm density, assuming that multithread channel networks may breach the same berm more than once. In some cases, small clusters of laterally discontinuous berms were found; these complexes were counted as one berm each.

3.2. Remote data collection

United States Geological Survey (USGS) 3DEP 1-m digital elevation models (DEMs) were sourced from OpenTopography for elevation and topographic data. Coupled satellite imagery and fieldwork were used to delineate bead lateral extent. Total valley width in incised systems was generally not reflective of active floodplain width, necessitating the additional use of DEMs to distinguish between active floodplain and inactive low terraces. ArcGIS Pro Version 3.3.1 (ESRI Inc., 2024) and Google Earth Pro were used to estimate bead-scale geometric variables (bead area, bead slope, floodplain-channel width ratio) (Supplemental Fig. S5).

Elevation and contributing drainage area serve as proxies for total water input to the system. Convective rainstorms and resultant flash flooding are atypical above 2,300 m, and stream hydrographs above this elevation are generally dominated by snowmelt peak flows in late spring-early summer (Jarrett, 1990; Solander et al., 2018; Kornse and Wohl, 2020) unless a catchment-scale disturbance such as wildfire has altered rainfall-runoff characteristics (Triantafillou and Wohl, 2024). The USGS StreamStats Batch Processing Tool was used to calculate geomorphic variables influencing water inputs (catchment area, mean basin elevation, maximum basin elevation, minimum basin elevation, and outlet elevation, percentage of catchment over 2,300 m, percentage of forest cover in National Land Cover Database (NLCD) class 41–43 (Deciduous, Evergreen, and Mixed Forest)). All beads were found to be above the 2300 m elevation threshold, and thus this metric was deemed statistically irrelevant. The Batch Processing tool also provided estimated discharges of 2-year (50% Annual Exceedance Probability [AEP]) and 100-year floods (1% AEP), average yearly catchment precipitation, 100-year intensity 6-h precipitation (I6H100Y), and percentage of catchment with surface water storage (STORNHD).

Sediment input was evaluated via the proxies of catchment wildfire burn severity and average catchment slope. Post-fire sediment yields are typically orders of magnitude greater than sediment yields in the Front Range under non-fire or background conditions (Ryan et al., 2024; Moody and Martin, 2001) and vary spatially by slope and severity within burn scars (Pelletier and Orem, 2014). Burn severity was assessed with dNBR (Δ Normalized Burn Ratio) and severity classes adapted from Rakholia et al. (2020). Thirty-meter Landsat 8 Collection-2 Level-2 satellite imagery from early July 2020 and early September 2021 were used as pre- and post-fire data. Imagery was selected for minimal cloud cover and for capturing spring/summer riparian spatial footprint. Pre-fire NBR and post-fire NBR rasters were created in ENVI Version 6.0 (NV5 Geospatial, 2023), and ArcGIS Pro produced the finalized output differencing the two rasters. Zonal histograms quantified severity distributions across the entire burn scar, summarized into three metrics for each catchment: the proportion of the catchment burned at high severity (dNBR >0.66), the proportion of the catchment burned, and the proportion of high severity burn to total burn.

3.2.1. Functionality responses

Normalized Difference Vegetation Index (NDVI) and Normalized Difference Water Index (NDWI) measure floodplain greenness and wetness, respectively, both of which are indicators of floodplain-channel connectivity and thus bead functionality (Fairfax and Whittle, 2020; Thomas et al., 2015) and serve as a proxy for increased storage in beads. NDWI was calculated with the methodology outlined by McFeeters (1996) to characterize surface water extent. PlanetScope 3-m RGB-NIR imagery from July 2021 was used to calculate NDVI and NDWI. Imagery timing avoided the months immediately post-fire as well as anomalously wet conditions. NDVI and NDWI rasters and summary statistics (mean, minimum, maximum, and range) were calculated in ArcGIS Pro.

Spatial heterogeneity was evaluated through patch density as an indirect indicator of bead storage capability by identifying distinct vegetation communities and structures, or patches, in the channel and floodplain that alter river response to disturbance and improve attenuation of fluxes through an increase in complexity and hydraulic roughness (Wohl and Iskin, 2022). Patches are typically delineated to capture variations in vegetation reflecting substrate grain size, soil moisture, and relative elevation. Patches were identified through field observation (Fig. 6), delineated in Google Earth Pro, and analyzed in ArcGIS Pro (Supplemental Fig. S4). The target metric, patch density, was calculated as the number of patches per square kilometer of bead area. The number

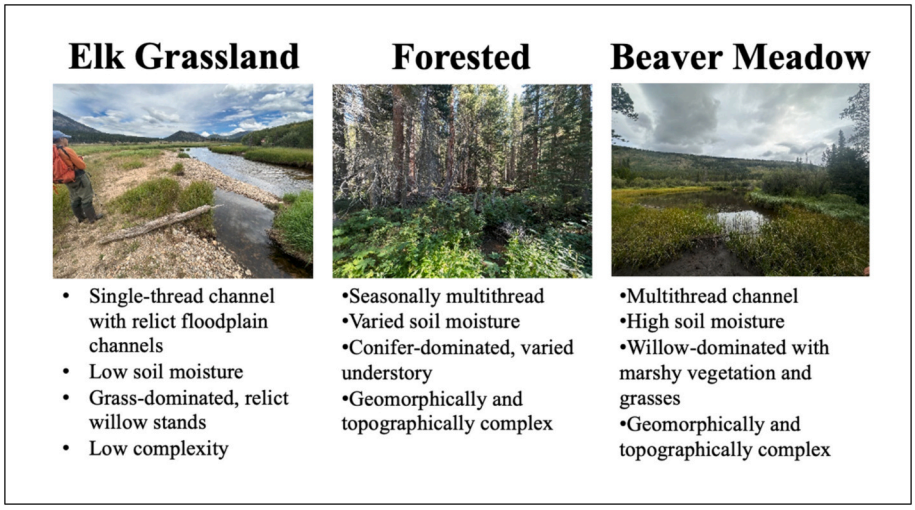

Fig. 5. Bead characteristics that likely contribute to differences in functionality. From left to right: Big Thompson River, North St. Vrain River, and Glacier Creek. Photos taken by Katie Larkin in Summer 2024.

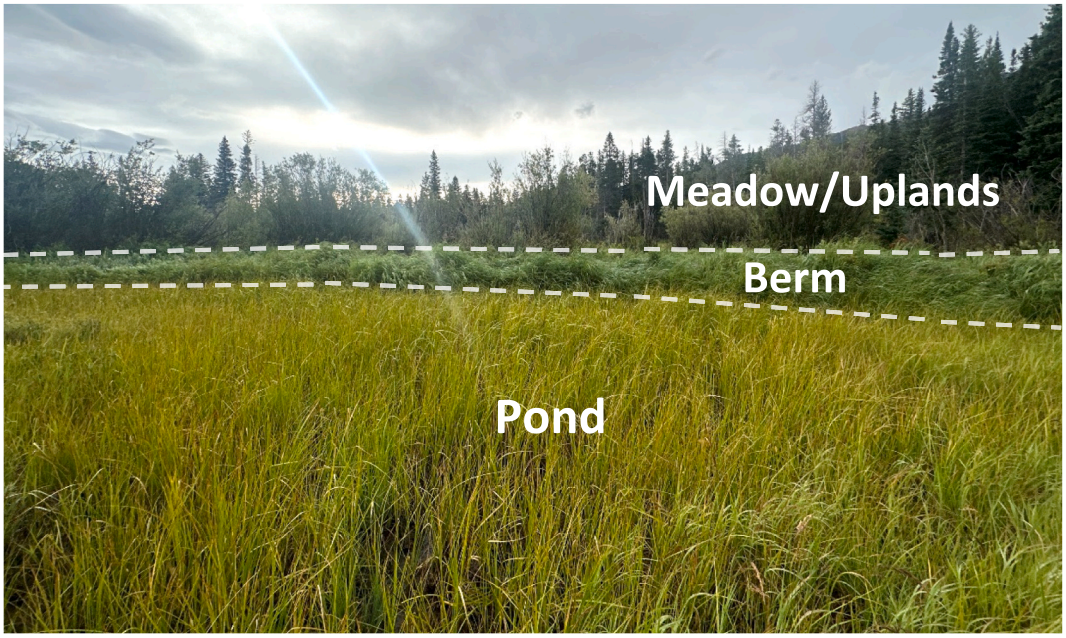

Fig. 6. Vegetation and topographic contrasts contributing to patchiness at Glacier Creek. In this beaver meadow bead, the foreground is a relict pond now covered with hydrophytic vegetation, the relict berm crest is ~1.5 m higher than the pond, and the background portion of the bead in this view is covered with willows. These three domains (pond, berm, and meadow/uplands) and all continuous land within them are considered individual patches. Photo taken by Katie Larkin in Summer 2024.

of continuous patches was also counted for each bead. Minimum patch size was 1 square meter, on the assumption that DEM and satellite imagery spatial resolutions were not suitable for finer detail. Supplemental Table S1 describes patch types and examples.

Total sinuosity, or the ratio of primary and secondary channel length to valley length, can be used as an indicator of bead attenuation potential. Sinuous and complex channel systems facilitate slowing of water and deposition of sediment; straight channel reaches do not as readily reduce or vary water velocity or encourage retention of materials (Wohl and Iskin, 2022). Sinuosity can differentiate between strings and beads; smaller floodplain-channel width ratios decrease lateral channel mobility, and thus these reaches generally have lower channel sinuosity than beads. In addition to the sinuosity of the active channel, rivers with high rates of lateral mobility will carve and abandon channels over time; these relict channels create topographic relief in the floodplain and increase patchiness. Highly sinuous channels may also create additional floodplain heterogeneity, when chutes and small passages erode paths of lesser resistance between large bends. Valley and primary/secondary channel lengths were calculated in Google Earth Pro.

3.3. Statistical analyses

All statistical analyses were completed using R version 4.4.3 in R Studio, and all tests were run at a significance level of $\alpha = 0.05$. All variables were assessed for normality of distribution using Shapiro-Wilk's Tests and transformations were performed where necessary to approximate normal distributions. Several variables could not be transformed to achieve normality using those methods and were

assessed with non-parametric tests.

Bead categories were assigned under the assumption that each will have different levels of functionality based on dominant vegetation and spatiotemporal distributions of water and sediment in the channel, or timing and nature of geomorphically significant flows. Each bead was grouped two times, by vegetation type (beaver meadow, forest, or elk grassland) and elevation zone (montane or subalpine). Bead type was established using the criteria in Section 3.1 and elevation zone was assigned using the elevation stratifications from Veblen and Donnegan (2006).

Categorical analysis tested the statistical significance of the two categories and attempted to characterize naturally occurring groups within predictors and responses (Table 1). Transformed variables were tested with one-way analysis of variance (ANOVA) to locate statistically significant differences by category (i.e., does bead size vary by category). Tukey Honest Significant Difference (HSD) tests returned metrics for pairwise comparisons between categories (i.e., beaver meadow – elk grassland). Nonparametric variables were tested with Kruskal-Wallis Rank Sum Tests and Dunn's test with Bonferroni-adjusted *p*-values. Elevation zone did not meet the criteria for Kruskal-Wallis and Dunn analysis, which requires at least 3 factors for pairwise comparison. Transformed variables in this category were analyzed with two-sample *t*-tests and nonparametric variables were assessed with Mann-Whitney *U* Tests.

Multiple linear regressions (MLRs) quantified the relative impacts of select driver variables on each response variable and produced a series of models helping to explain and/or predict functionality. These models also helped identify certain factors to be dismissed through lack of correlation with bead functionality. Beads were considered as individual units and signal propagation between them was not accounted for. Prior to MLR analysis, correlation matrices quantified weightedness of relationships between all driver variables, and any confounding relationships were not included in models.

Backward and forward stepwise linear regression were used to select model variables. Corrected Akaike's Information Criterion (AICc), a model fittedness metric developed for small dataset sample size, large number of parameters, and penalization of overfitting (Hurvich and Tsai, 1989), was used for best-fit model selection. Models with the smallest AICc were selected as best-fits. All best-fit models were assessed for statistical significance and checked for acceptable use via the assumptions of homogeneity, linearity, and normality.

A total of six models (NDVI mean and range, NDWI mean and range, patch density, total sinuosity) were generated, but NDVI and NDWI mean models will not be discussed further. We decided that NDVI and NDWI mean models, by reducing conditions to a single representative number, did not adequately reflect the heterogeneity that we associate with functional beads. NDWI mean and range, patch density, and total sinuosity models were generated twice, once including categories as a potential driver variable and once excluding categories. The model selection process remained the same for both scenarios.

4. Results

We first summarize the range of bead characteristics in the dataset (Table 2). We then describe the results of categorical analyses of bead types and beads in different elevation zones, undertaken to test hypothesis one. Finally, we present the results of statistical models of driver and response variables for bead functionality, which were used to test hypotheses two and three. Supplemental Tables S2 through S7 provide individual bead locations and descriptive data.

4.1. Categorical analysis

Categorical analysis was performed successfully for groupings of variables by bead type and by elevation zone (Table 3). Supplemental Tables S8 and S9 provide comparison results for vegetation type and elevation zone, respectively. Testing for statistical significance revealed significant relationships for individual variables as well as between categorical levels as pairwise comparisons for both categories. Categorizing beads by type was statistically significant for 23 of the 30 predictor and response variables investigated. Pairwise comparisons between beaver meadows and elk grasslands, beaver meadows and forested beads, and forested beads and elk grasslands were statistically significant for 10, 14, and 12 predictor and response variables, respectively. Categorizing beads by elevation zone was statistically significant for 10 of the 30 predictor and response variables investigated. These results generally support *H1* in demonstrating that river bead functionality proxies differ in relation to bead type and elevation zone.

Table 2
Summary of bead characteristics in the dataset.

Variable	Mean value	Range
Bead size	0.072 km^2	0.00133 to 0.452 km^2
Bead slope	0.034	0.0036 to 0.109
Ratio of floodplain width to channel width	59.8	3.8 to 517.1
Bead ratio	0.006	0.0000425 to 0.043
Catchment drainage area	24.86 km^2	0.36 to 233.9 km^2
Average catchment slope	0.163	0.0586 to 0.292
Average catchment elevation	3,070 m	2,548 to 3,544 m
Mixed forest percent	67.3%	13.6 to 98.4%
Berm density	19.8 berms/km	0 to 67.3 berms/km
Minimum berm count	24	0 to 359
Wood density	120 pieces/km	0 to 1390 pieces/km
I6H100Y (6-h precipitation that occurs on average every 100 years)	73 mm	51 to 83 mm
1% annual exceedance probability (AEP)	7.0 m^3/s	0.34 to 35.4 m^3/s
50% AEP	2.85 m^3/s	0.077 to 17.4 m^3/s
Mean annual precipitation	671 mm/yr	428 to 1,144 mm/yr
Total percent of catchment surface water storage (STORNHD)	0.48%	0 to 2%
High severity burn percent (HSB)	9.3%	0 to 40.6%
Total burn percent (TB)	46.2%	0.3 to 95.3%
Burn ratio (BR)	0.18	0 to 0.51
NDVI	0.402	0.051 to 0.569
NDWI	−0.71	−0.95 to −0.39
Patch count	38	3 to 131
Patch density	3806 patches/km	19 to 41,469 patches/km
Total sinuosity	1.51	1.01 to 3.04

Vegetation type was the most statistically successful category used to group beads. Vegetation types differed most in relation to spatial density of large wood and maximum NDWI. Forested beads had greater wood density and elk grasslands had the lowest wood density. All three pairwise comparisons (EG-F, F-BM, BM-EG) were significant for these two metrics, indicating that each bead type is statistically distinct in the context of these variables. Partial distinctness (significance of 2 pairwise comparisons) was observed for (i) bead size, with elk grasslands being larger than other beads; (ii) 50% AEP, with elk grasslands and forested beads having greater estimated 2-year peak discharges and subalpine beads having greater discharges than montane; (iii) NDVI range and NDWI range, with elk grasslands having greater ranges than other bead types; and (iv) patch count and patch density, with beaver meadows having greater patch count and density and montane beads having greater patch density. All other variables were either insignificant when examined by type or had one significant pairwise comparison.

4.2. Bead functionality statistical models

Strength of association between predictor variables was examined prior to the model selection process (Supplemental Tables S10 and S11). Moderate to high statistically significant positive correlation (>0.6) was

Table 3
Summary of significant relationships between predictor/response variables and categories. An "X" signifies a significant ($p < 0.05$) relationship. EG = elk grassland, BM = beaver meadow, F = forested, Mont = montane, and Sub = subalpine.

Variable	Veg. Type	Elevation Zone	Relationship(s)
Bead Size	X		EG > F and BM
Bead Slope	X		F > EG
Floodplain-Channel Width Ratio	X	X	BM > F, Mont > Sub
Bead Ratio	X		EG > F
Catchment Size	X		EG > BM
Average Catchment Slope	X	X	F > BM and EG, Sub > Mont
Average Catchment Elevation	X	X	F > BM and EG, Sub > Mont
Mixed Forest	X	X	BM > F, Mont > Sub
Berm Density	X		BM > F
Minimum Berm Count			N/A
Wood Density	X		F > BM > EG
I6H100Y	X		F > EG
1% AEP	X	X	EG > BM, Sub > Mont
50% AEP	X	X	EG and F > BM, Sub > Mont
Precipitation	X	X	F > BM, Sub > Mont
STORNHD			N/A
High Severity Burn			N/A
Total Burn		X	Mont > Sub
Burn Ratio	X		F > BM
Minimum NDVI	X		F and BM > EG
Maximum NDVI			N/A
Average NDVI			N/A
NDVI Range	X		EG > F and BM
Minimum NDWI	X	X	BM > F, Mont > Sub
Maximum NDWI	X		EG > BM > F
Average NDWI	X		F > EG and BM
NDWI Range	X		EG > F and BM
Patch Count	X		BM > EG > F
Patch Density	X	X	BM > EG, Mont > Sub
Total Sinuosity			N/A

found between: bead size and 1% AEP (0.67), 50% AEP (0.63), and minimum berm count (0.67); average catchment slope and 50% AEP (0.63), average catchment elevation (0.82), and precipitation (0.81); drainage area and 1% AEP (0.8) and 50% AEP (0.66), STORNHD and average catchment elevation (0.64); 1% AEP and 50% AEP (0.97); and precipitation and 50% AEP (0.61) and average catchment elevation (0.81). All correlations were statistically significant with $p < 0.05$. Moderate to high statistically significant negative correlation (<−0.6) was found between: average catchment slope and total burn (−0.66) and mixed forest percent (−0.77); total burn and average catchment elevation (−0.64) and precipitation (−0.65); and mixed forest percent and STORNHD (−0.63), average catchment elevation (−0.82), and precipitation (−0.77). All correlations were statistically significant with $p < 0.05$. Given the number of statistically significant correlations between predictors, models were also assessed for multicollinearity via Variable Inflation Factor (VIF). A VIF of over 5 is generally considered large and necessitates adjustment or removal of predictor variables in the model. Checks for linearity, homogeneity, and normality revealed no violations among any of the selected models.

The NDVI range model with the lowest AICc contains bead ratio, bead slope, mixed forest percent, I6H100Y and type (Table 4). This model is statistically significant (F-statistic = 9.5, $p < 0.001$) and has an AICc of 30.4. This model implies a positive relationship with bead ratio, a negative relationship with bead slope, a slight negative relationship with mixed forest percent, and a slight positive relationship with I6H100Y, with the highest NDVI ranges in elk grasslands, and the lowest in forested beads. Bead ratio and bead slope are not statistically significant in the model.

The NDWI range model with the lowest AICc contains bead ratio, bead slope, burn ratio, mixed forest percent, I6H100Y, and type (Table 5). This model is statistically significant (F-statistic = 10.9, $p < 0.001$) and has an AICc of −130.1. This model implies a positive relationship with bead ratio, a slight positive relationship with burn ratio and I6H100Y, a negative relationship with bead slope, a slight negative relationship with mixed forest percent, highest NDWI ranges in elk grasslands, and lowest in forested beads. Burn ratio is not statistically significant in the model.

Table 4
Model statistics and AICc for functionality drivers and NDVI range; bolded text indicates the preferred model.

Variable	Terms	p-value	AICc
NDVI Range	**BeadRatio + BeadSlope + MixedForestPct + 16H100Y + factor(Type)**	<0.001	**30.5**
NDVI Range	BeadRatio + MixedForestPct + XI6H100Y + factor(Type) + TotalBurnPct	<0.001	34.3
NDVI Range	BeadRatio + factor(Type) + BermDensity	<0.001	49.6
NDVI Range	factor(Type) + BeadRatio + MixedForestPct	<0.001	35.8
NDVI Range	BeadSlope + MixedForestPct + XI6H100Y + factor(Type) + FPCR	<0.001	33.6

The patch density model with the lowest AICc contains type, berm density, bead ratio, 1% AEP, and minimum berm count (Table 6). This model is statistically significant (F-statistic = 29.0, $p < 0.001$) and has an AICc of 115.1. This model implies a strong negative relationship with bead ratio, slight negative relationships with 1% AEP and minimum berm count, and a slight positive relationship with berm density.

The total sinuosity model with the lowest AICc contains average catchment slope, average catchment elevation, and elevation zone (Table 7). This model is statistically significant (F-statistic = 6.0, $p = 0.0015$) and has an AICc of −15.2.

The models for each functionality indicator support *H2* in that river bead functionality consistently correlates more strongly with multiple potential driver variables than with any single variable. The models also mostly support *H3* in that bead size correlates significantly with three of the four functionality metrics.

Models were also run a second time excluding categories (vegetation type and elevation zone) as driver variables (Table 8) for all functionality proxy variables to assess patterns within the entire dataset. Three of the four models changed. The model for patch density remained the same; the most significant driver variables explaining variations in patch density, regardless of category, are bead ratio, berm density, 100-year flood (X1pctAEP), and minimum berm count. Comparing the models for NDVI and NDWI range with categories to the models without categories, maximum 6-h precipitation (I6H100Y) is no longer significant but the 100-year flood and wood density become significant in each model. For NDWI range, burn ratio and mixed forest percent are no longer significant without categories, but average catchment slope becomes significant. The greatest change is in the model for total sinuosity,

Table 5
Model statistics and AICc for functionality drivers and NDWI range; bolded text indicates the preferred model.

Variable	Terms	p-value	AICc
NDWI Range	**BeadRatio + BeadSlope + BurnRatio + MixedForestPct + I6H100Y + factor(Type)**	<0.001	**−130.1**
NDWI Range	1pctAEP + BeadRatio + BeadSlope + AvgCatchSlope + factor(Type) + TotalBurnPct + Precip	<0.001	−124.9
NDWI Range	BeadSlope + Precip + factor(Type) + BermDensity +1pctAEP + BeadRatio	<0.001	−123.0
NDWI Range	BeadRatio + BeadSlope + MixedForestPct + XI6H100Y + factor(Type)	<0.001	−128.7
NDWI Range	BeadRatio + BeadSlope + MixedForestPct + XI6H100Y + factor(Type) + WoodDensity	<0.001	−126.2

Table 6
Model statistics and AICc for functionality drivers and patch density; bolded text indicates the preferred model.

Variable	Terms	p-value	AICc
Patch Density	**BermDensity + BeadRatio + X1pctAEP + MinBermCount**	<0.001	**115.1**
Patch Density	BermDensity + Precip + BeadRatio + X1pctAEP + MinBermCount + factor(Status)	<0.001	118.2
Patch Density	BermDensity + Precip + BeadRatio + X1pctAEP + MinBermCount	<0.001	116.3
Patch Density	factor(Type) + BermDensity + Precip + BeadRatio +1pctAEP + MinBermCount + factor (Status)	<0.001	119.8
Patch Density	BermDensity + Precip + BeadRatio + X1pctAEP + MinBermCount + factor(Type)	<0.001	117.9

Table 7
Model statistics and AICc for functionality drivers and total sinuosity; bolded text indicates the preferred model.

Response Variable	Model Terms	p-value	AICc
Total Sinuosity	**AvgCatchSlope + AvgBasinElev + factor (ElevationZone)**	**0.0015**	**−15.2**
Total Sinuosity	BeadRatio + AvgCatchSlope + AvgBasinElev + factor(ElevationZone)	0.0042	−12.7
Total Sinuosity	AvgCatchSlope + TotalBurnPct + AvgBasinElev + factor(ElevationZone)	0.0016	−15.0
Total Sinuosity	AvgBasinElev + factor(ElevationZone) + MixedForestPct + AvgCatchSlope	0.0036	−13.0
Total Sinuosity	BeadSlope	0.039	−8.0

in which the significant predictor variables change completely.

5. Discussion

For all four evaluated functionality proxy variables, regressions showed greater statistical validity of multivariate models over univariate models. All models that included bead categories had at least two statistically significant variables of interest. Despite varied coefficients and effects, it is evident that functionality reflects complex interactions among multiple variables. Categorical comparisons displayed significant differences in bead/catchment geometry, driver variables, and perceived functionality by dominant vegetation and elevation, with vegetation type being the most successful discriminator. Vegetation type differs significantly between elk grasslands, beaver meadows, and forested beads with respect to catchment/bead geometry, magnitude of inputs, and magnitude of responses. Elevation zone primarily captured inherent differences in geometry and regional hydrology between montane and subalpine beads but also identified a relationship between elevation and level of channel confinement.

The influence of multiple variables on river bead functionality supports our second hypothesis. The specific driver variables that we included in our analyses reflect the biogeographic characteristics of the study area. Other variables might create more important influences on river bead functionality in other biogeographic regions. In catchments that are not forested and do not have beavers, for example, or that are driven primarily by groundwater inputs, it would be appropriate to choose different driver variables.

5.1. Model outputs and implications

The best statistical models that included bead categories for the functionality proxies of NDVI range, NDWI range, patch density, and total sinuosity differed in the variables selected, the strength of individual variable influence in each model, and the number of significant variables (Supplemental Tables S12-S14). Bead ratio, or the ratio of bead size to catchment size, appeared in three of the four models, the most of any variable, suggesting that the catchment-bead size relationship is of primary importance in determining functionality. Coefficients for one of these three models (NDVI range) were not significant, but the significance of the entire model ($p < 0.001$) fails to disprove the possibility that bead ratio influences NDVI. Patch density was influenced primarily by bead ratio; lower bead ratios, or smaller beads relative to catchment size, are strongly associated with high patch densities. Larger bead ratios were associated with higher NDVI and NDWI ranges. Aside from bead ratio, some drivers (bead slope, mixed forest percentage, 100-year precipitation (I6H100Y), and vegetation type) were present in more than one model. Certain variables were deemed insignificant or were detrimental to model performance; wood density, in particular, decreased model performance.

Bead ratio may successfully capture both relative magnitude of fluxes (assumed to increase with catchment size) and the available area for these fluxes to be attenuated. Significant positive relationships between catchment size and bead size ($p < 0.001$) as well as catchment size and average floodplain width ($p = 0.0046$) are intuitive given the likely increase in fluvial erosive power with increasing catchment size and discharge. However, the strong negative relationship between catchment size and floodplain-channel width ratio ($p < 0.001$) suggests that smaller streams (typically second- and third-order) have the highest proportion of accessible floodplain relative to their discharge. Beads in the subalpine region have significantly lower floodplain-channel widths although catchment size did not differ significantly by elevation zone, suggesting that differences in floodplain width between elevation zone may reflect factors other than catchment size. Lower values of total sinuosity and patch density in subalpine beads suggest that the greater lateral confinement of beads in this elevation zone may limit bead functionality by reducing lateral mobility.

Selected models mostly contained mixtures of geomorphic and biotic variables but tended to correlate most with geomorphic factors. Patch density was the only variable that strongly reflected biotic factors, particularly beaver modification. Geomorphic variables were measured on both catchment- and reach-scales, and biotic variables were typically only measured on the reach-scale. Within both scaled groupings of geomorphic inputs, catchment geometry and inputs tended to be selected over reach-scale geometry and inputs.

Excluding the categorical variables of elevation and bead type from models – a means of investigating patterns in the whole dataset - changed three of the four models. Category-included models preferred catchment-scale geomorphic inputs, but changes in models seemed to increasingly reflect reach-scaled biotic inputs. The patch density model was the only model that remained the same; although it differed significantly by vegetation type, it primarily reflects hydrologic inputs, catchment and reach geometry, and beaver modification. Total sinuosity changed from a multivariate model to a univariate model, containing

Table 8
Summary of differences between selected functionality models run with and without categories.

Variable	Model with categories	Model without categories
NDVI Range	BeadRatio + BeadSlope + MixedForestPct + I6H100Y + factor(Type)	X1pctAEP + BeadRatio + BeadSlope + MixedForestPct + WoodDensity
NDWI Range	BeadRatio + BeadSlope + BurnRatio + MixedForestPct + I6H100Y + factor(Type)	X1pctAEP + BeadRatio + BeadSlope + AvgCatchSlope + WoodDensity
Patch Density	BermDensity + BeadRatio + X1pctAEP + MinBermCount	NO CHANGE
Total Sinuosity	AvgCatchSlope + AvgBasinElev + factor(ElevationZone)	BeadSlope

only reach slope; in this model, a negative relationship between total sinuosity and reach slope may be attributed to known increases in incision, and thus single-threaded channel planform, with steeper channel slopes.

Category-excluded models for NDVI and NDWI range both included wood density, introducing the possibility that including bead categories in the model selection process broadened the focus of the models, reducing the signal emitted by variations in wood density between beads. In-channel wood is known to influence both deposition and scour (Gurnell et al., 2002; Wohl and Scott, 2017), which may complicate attenuation of downstream fluxes. Some large wood pieces or jams caused pool formation and sediment retention, whereas others facilitated the formation or migration of knickpoints and incision. We observed variable hydraulic effects at individual jams, resulting in complex bathymetry and geomorphic effects. Thus, it is difficult to generalize the effects of large wood in beads, and characterizing the geomorphic effects of large wood at smaller spatial scales may provide clearer insights into the effects of wood load on flux attenuation.

5.2. Implications for river restoration

Numerous methods of assessing and ranking hydromorphological functionality have been proposed since the 1980s. As reviewed by Belletti et al. (2015), these can be distinguished as focusing on physical or riparian habitat assessment, morphological assessment, or alteration of the hydrological regime. Examples include the River Styles framework (Brierley and Fryirs, 2000) and the morphological quality index (Rinaldi et al., 2013, 2015). These assessments may be focused on classifying or ranking functionality, as well as assessing potential evolutionary trajectories (Fryirs et al., 2012) of a river corridor. Our intent in this study was not so much to classify or rank the functionality of river beads but rather to evaluate the potential importance of different potential driver variables for functionality. Some of our driver variables, such as wood characteristics and riparian vegetation, have been used in previous work such as the morphological quality index.

Catchment- and reach-scale characteristics vary substantially between beads, making it difficult to provide universal recommendations for restoration techniques. Prior to restoration, however, we recommend that practitioners take care in the site selection process to evaluate existing conditions and potential for restoration. Consideration of fixed variables, such as slope, elevation, and floodplain-channel width ratio may facilitate selection of beads in which restoration can most effectively increase function (Wohl et al., 2024b). Beads with lower floodplain-channel width ratio or greater channel lateral confinement, for example, may not allow for increases in sinuosity and may not possess necessary space to support optimal levels of floodplain diversity.

Techniques for restoration vary by project depending on the physical template provided by the bead, as well as the goals of restoration practitioners and shareholders (e.g., Smith et al., 2014; Verdonschot and Verdonschot, 2023). Restoration techniques such as reconfiguring channel and floodplain topography or introducing obstacles to the channel to promote floodplain-channel connectivity (Powers et al., 2019; Flitcroft et al., 2022) are likely to increase bead functionality by promoting activation of secondary channels, greater flood-prone width, and increased storage and retention of water, sediment, and nutrients in the floodplain.

The positive relationship between berm density and patch density suggests that reintroduction of beaver, or structures simulating their presence, could lead to an improvement in functionality, as documented in other field sites (Pollock et al., 2007; Pearce et al., 2021; Puttock et al., 2021). Patch density is typically greater in smaller beads, which tended to have more closely spaced berms, as opposed to larger beads, which had greater numbers of berms but lower densities, as shown through a positive relationship between patch density and berm density ($p < 0.001$) and negative relationship between minimum berm count and patch density ($p = 0.014$).

Interpretations of the statistical models suggest factors that can aid in site interpretation and selection. Patch metrics and NDVI/NDWI may be concurrently used to assess the transition from hydrologically connected beaver meadows to hydrologically disconnected elk grasslands. As endmembers on a continuum, beaver meadows and elk grasslands both hosted a variety of patch types, typically the result of active or relict beaver activity and abandoned channel segments. However, NDVI and NDWI reveal differences in biology and subsurface hydrology that highlight differences in the degree of connectivity.

High patch density ($p = 0.0017$) in beaver meadows, coupled with a lower NDVI range ($p < 0.001$) and NDWI range ($p < 0.001$), indicates that, despite variations in surface topography and vegetation, hydrologic conditions were less variable. Except for small areas at higher elevations, patches in beaver meadows are associated with high soil moisture levels and retention of water. Elk grasslands, despite significantly lower patch densities, were coupled with a high NDVI/NDWI range, illustrating systemic disconnectivity that manifests most clearly through variations in surface topography and vegetation (Fig. 7). Grass and highland patches typically contain lower soil moisture, whereas abandoned channels and remnant beaver berms are associated with surface water retention and increased soil moisture. Beaver meadows and elk grasslands did not have statistically significant differences in average NDVI and NDWI, but NDVI/NDWI ranges and visual cues from satellite imagery and fieldwork support the interpretation of greater wetness and surface water ponding in beaver meadows. Combined patch metrics and NDVI/NDWI may be used as pre-selection to assess conditions prior to emplacement of restoration strategies, or as a monitoring tool to examine spatiotemporal changes in hydrologic connectivity.

6. Conclusions

Our assessment of proxy metrics for the potential for attenuation of downstream fluxes of water, sediment, and other materials in river beads suggests that attenuation correlates most strongly with bead ratio, or the ratio of bead size to catchment size. The potential for flux attenuation tends to be greatest in beads with small ratios. Total sinuosity was not associated with bead ratio, but lower floodplain-channel width ratios in subalpine beads correspond to lower total sinuosity, likely as a byproduct of insufficient stream corridor width to support multithread channels. Relationships between functionality response variables and geomorphic and biotic driver variables suggest that functionality is most influenced by geomorphic variables, particularly those measured at the catchment scale. However, patch density is almost exclusively biotically driven because of the strong correlation with beaver berms.

Beads, although influenced by regionally scaled relationships like drainage area-discharge, are generally the unique products of their physical settings, the inputs they receive, and, to some extent, alterations to the stream corridors and uplands from human and natural disturbances. Categorizing beads to reflect observable differences in their dominant vegetation type and elevation zone indicates significant differences in form and function in both cases. In particular, vegetation type reflects hydrologic connectivity associated with ecosystem degradation in beads. The transition from beaver meadows (willow-dominated) to elk grasslands (grass-dominated) marks a transition from high hydrologic connectivity between channel and floodplain to an incised, disconnected state. High patch density and low NDVI/NDWI range in beaver meadows reflect physical heterogeneity and consistent greenness/wetness. Low patch density and high NDVI/NDWI range in elk grasslands reflect loss of heterogeneity and an impaired state in which remaining topographic low areas in the stream corridor can become hydrologically disconnected during base flow. Forested beads, which are not part of this transitional relationship, are a unique habitat of their own. Adjusting functionality models to exclude these categories caused a slight shift in model preference from geomorphic to biotic and reach-scale variables.

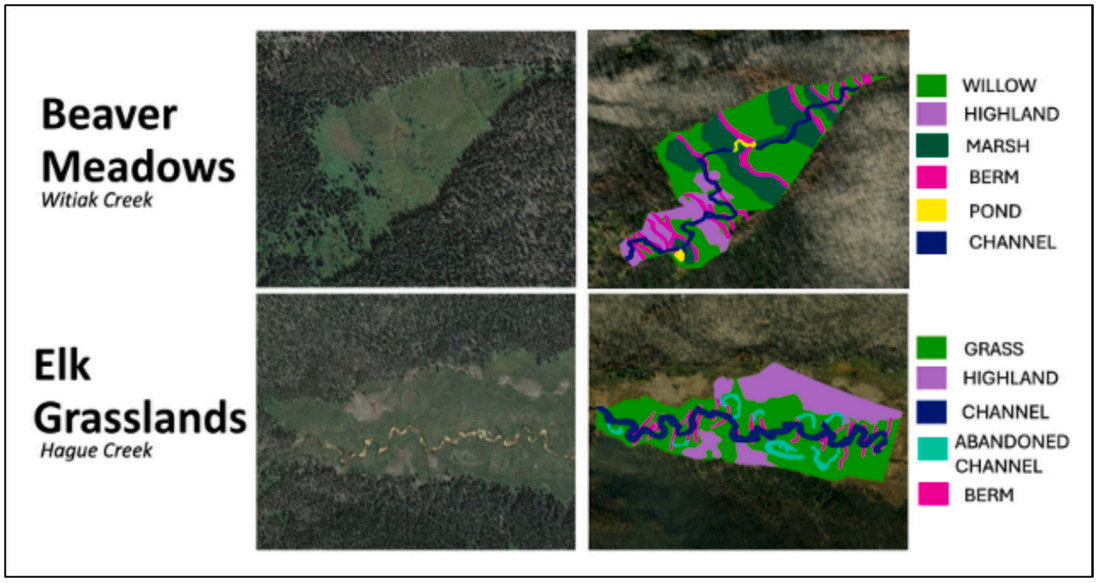

Fig. 7. Variations in bead patch types between beaver meadows and elk grasslands, as seen for Witiak Creek and Hague Creek. Imagery provided by Google Earth Pro (Landsat/Copernicus, 2025) and ArcGIS Pro (ESRI, 2024).

Certain factors controlling bead functionality, such as absolute bead size, cannot be modified, but functionality is a dynamic metric reflecting the geomorphic and biotic variables that influence flux attenuation. We expect the variables used in this analysis to be relevant to this study area regardless of disturbance history, but the details of disturbance history may strongly influence the specific values of some variables. In other words, potential drivers such as wood load or riparian buffer might change after wildfire and response variables such as patch density might change quickly following beaver colonization of a river bead.

Statistical analyses did not suggest a clear or immediate route for addressing functionality in a restoration context. However, the correlation between bead ratio and nearly all measures of functionality suggests that recapturing natural floodplain extent and restoration of connectivity would increase functionality as reflected in the potential for attenuation of downstream fluxes of materials. Strategies that will improve water retention and lead to floodplain inundation and alteration from incised, single-thread channel planform to a multithread planform will likely create the most measurable improvements in bead functionality.

CRediT authorship contribution statement

Katie Larkin: Writing – review & editing, Writing – original draft, Visualization, Methodology, Investigation, Formal analysis, Conceptualization. **Ellen Wohl:** Writing – review & editing, Methodology, Investigation, Funding acquisition, Formal analysis, Conceptualization.

Declaration of competing interest

The authors declare the following financial interests/personal relationships which may be considered as potential competing interests: Katie Larkin reports financial support was provided by USDA. Katie Larkin reports financial support was provided by Geological Society of America. If there are other authors, they declare that they have no known competing financial interests or personal relationships that could have appeared to influence the work reported in this paper.

Acknowledgements

Funding provided by USDA Forest Service Agreement No. 23-CS-11221634-046, a Geological Society of America Graduate Student Research Grant, and the Warner College of Natural Resources at Colorado State University. Thank you to Shayla Triantafillou, Owen Richardson, Aaron Katz, and Alissa Larkin for their help in the field; to Taryn Contento, Anna Cloud, Larry Dale, and Scot Barker for site-specific assistance; to Bridget Livers for supplementary data; and to Eric Gilleland for help with statistical analyses. The manuscript benefited from comments by two anonymous reviewers.

Appendix A. Supplementary data

Supplementary data to this article can be found online at https://doi.org/10.1016/j.geomorph.2026.110297.

Data availability

Data are available in Mendeley Data Repository with DOI: 10.17632/xx66nsvk56.1

References

Appling, A.P., Bernhardt, E.S., Stanford, J.A., 2014. Floodplain biogeochemical mosaics: a multidimensional view of alluvial soils. J. Geophys. Res. Biogeosci. 119, 1538–1553. https://doi.org/10.1002/2013JG002543.

Barinas, G., Good, S.P., Tullos, D., 2024. Continental scale assessment of variation in floodplain roughness with vegetation and flow characteristics. Geophys. Res. Lett. 51 (1), e2023GL105588. https://doi.org/10.1029/2023GL105588.

Belletti, B., Rinaldi, M., Buijse, A.D., Gurnell, A.M., Mosselman, E., 2015. A review of assessment methods for river hydromorphology. Environ. Earth Sci. 73, 2079–2100. https://doi.org/10.1007/s12665-014-3558-1.

Bellmore, J.R., Baxter, C.V., 2014. Effects of geomorphic process domains on river ecosystems: a comparison of floodplain and confined valley segments. River Res. Appl. 30 (5), 617–630. https://doi.org/10.1002/rra.2672.

Benson, L., Madole, R., Landis, G., Gosse, J., 2005. New data for late Pleistocene Pinedale alpine glaciation from southwestern Colorado. Quat. Sci. Rev. 24 (1–2), 49–65. https://doi.org/10.1016/j.quascirev.2004.07.018.

Beschta, R.L., Ripple, W.J., 2009. Large predators and trophic cascades in terrestrial ecosystems of the western United States. Biol. Conserv. 142 (11), 2401–2414. https://doi.org/10.1016/j.biocon.2009.06.015.

Biron, P.M., Buffin-Bélanger, T., Larocque, M., Choné, G., Cloutier, C.A., Ouellet, M.A., Demers, S., Olsen, T., Desjarlais, C., Eyquem, J., 2014. Freedom space for rivers: a sustainable management approach to enhance river resilience. Environ. Manag. 54, 1056–1073. https://doi.org/10.1007/s00267-014-0366-z.

Bouwes, N., Weber, N., Jordan, C.E., Saunders, W.C., Tattam, I.A., Volk, C., Wheaton, J. M., Pollock, M.M., 2016. Ecosystem experiment reveals benefits of natural and simulated beaver dams to a threatened population of steelhead (*Oncorhynchus mykiss*). Sci. Rep. 6 (1), 28581. https://doi.org/10.1038/srep28581.

Brierley, G.J., Fryirs, K., 2000. River Styles, a geomorphic approach to catchment characterization: implications for river rehabilitation in Bega catchment, New South

Wales, Australia. Environ. Manag. 25, 661–679. https://doi.org/10.1007/s002670010052.
Butler, D.R., Malanson, G.P., 2005. The geomorphic influences of beaver dams and failures of beaver dams. Geomorphology 71 (1–2), 48–60. https://doi.org/10.1016/j.geomorph.2004.08.016.
Chapman, S.S., Griffith, G.E., Omernik, J.M., Price, A.B., Freeouf, J., Schrupp, D.L., 2006. *Ecoregions of Colorado* (Color Poster with Map, Descriptive Text, Summary Tables, and Photographs). U.S. Geological Survey, Reston, Virginia (map scale 1:1,200,000).
Christensen, N., Morrison, R.R., 2026. The relative importance of floodplain storage and flow path dispersion on flood attenuation in mountain streams. Water Resour. Res. 62, e2024WR039628. https://doi.org/10.1029/2024WR039628.
Clarke, S.J., 2025. Full floodplain connectivity: realising opportunities for 'stage 0' river restoration. River Res. Appl. 41, 152–158. https://doi.org/10.1002/rra.4283.
Daniels, M.D., Rhoads, B.L., 2003. Influence of a large woody debris obstruction on three-dimensional flow structure in a meander bend. Geomorphology 51, 159–173. https://doi.org/10.1016/S0169-555X(02)00334-3.
DeBoer, J.A., Thoms, M.C., Delong, M.D., Parsons, M.E., Casper, A.F., 2020. Heterogeneity of ecosystem function in an "Anthropocene" river system. Anthropocene 31, 100252. https://doi.org/10.1016/j.ancene.2020.100252.
Dittbrenner, B.J., Schilling, J.W., Torgersen, C.E., Lawler, J.J., 2022. Relocated beaver can increase water storage and decrease stream temperature in headwater streams. Ecosphere 13 (7), e4168. https://doi.org/10.1002/ecs2.4168.
Dunn, S.B., Rathburn, S.L., Wohl, E., 2024. Post-fire sediment attenuation in beaver ponds, Rocky Mountains, CO and WY, USA. Earth Surf. Process. Landf. 49 (13), 4340–4354. https://doi.org/10.1002/esp.5970.
Ehlen, J., Wohl, E., 2002. Joints and landform evolution in bedrock canyons. Trans. Japanese Geomorphol. Union 23 (2), 237–255.
ENVI Version 6.0, 2023. NV5 Geospatial Software Documentation Center. NV5 Global, Inc.
ESRI Inc., 2024. ArcGIS Pro (Version 3.3.1). https://www.esri.com/en-us/arcgis/products/arcgis-pro/overview.
Fairfax, E., Whittle, A., 2020. Smokey the Beaver: Beaver-dammed riparian corridors stay green during wildfire throughout the western United States. Ecol. Appl. 30 (8), e02225. https://doi.org/10.1002/eap.2225.
Feio, M.J., Alves, T., Boavida, M., Medeiros, A., Graca, M.A.S., 2010. Functional indicators of stream health: a river-basin approach. Freshw. Biol. 55, 1050–1065. https://doi.org/10.1111/j.1365-2427.2009.02332.x.
Flitcroft, R.L., Brignon, W.R., Staab, B., Bellmore, J.R., Burnett, J., Burns, P., Cluer, B., Giannico, G., Helstab, J.M., Jennings, J., Mayes, C., Mazzacano, C., Mork, L., Meyer, K., Munyon, J., Penaluna, B.E., Powers, P., Scott, D.N., Wondzell, S.M., 2022. Rehabilitating valley floors to a stage 0 condition: a synthesis of opening outcomes. Front. Environ. Sci. 10, 892268. https://doi.org/10.3389/fenvs.2022.892268.
Fryirs, K., Brierley, G.J., Erskine, W.D., 2012. Use of ergodic reasoning to reconstruct the historical range of variability and evolutionary trajectory of rivers. Earth Surf. Process. Landf. 37, 763–773. https://doi.org/10.1002/esp.3210.
Fryirs, K.A., Brierley, G.J., Preston, N.J., Kasai, M., 2007. Buffers, barriers, and blankets: the (dis)connectivity of catchment-scale sediment cascades. Catena 70, 49–67. https://doi.org/10.1016/j.catena.2006.07.007.
Fryirs, K.A., Wheaton, J.M., Brierley, G.J., 2016. An approach for measuring confinement and assessing the influence of valley setting on rivers forms and processes. Earth Surf. Process. Landf. 41, 701–710. https://doi.org/10.1002/esp.3893.
Gambill, I., Marshall, A., Benson, D.A., McFadden, S., Navarre-Sitchler, A., Wohl, E., Singha, K., 2025. Exploring the influence of morphologic heterogeneity and discharge on transient storage in stream systems: 1. Insights from the field. Water Resour. Res. 61 (1), e2023WR036031. https://doi.org/10.1029/2023WR036031.
Google Earth Pro (2025) Google Earth LLC. https://earth.google.com/web/.
Graf, W.L., 2001. Damage control: restoring the physical integrity of American rivers. Ann. Assoc. Am. Geogr. 91, 1–27. https://doi.org/10.1111/0004-5608.00231.
Green, K.C., Westbrook, C.J., 2009. Changes in riparian area structure, channel hydraulics, and sediment yield following loss of beaver dams. Journal of Ecosystems and Management 10, 68–79. https://doi.org/10.22230/jem.2009v10n1a412.
Gurnell, A.M., 1998. The hydrogeomorphological effects of beaver dam-building activity. Progress in Physical Geography: Earth and Environment 22 (2), 167–189. https://doi.org/10.1177/030913339802200202.
Gurnell, A.M., Piegay, H., Swanson, F.J., Gregory, S.V., 2002. Large wood and fluvial processes. Freshw. Biol. 47, 601–619. https://doi.org/10.1046/j.1365-2427.2002.00916.x.
Hahn, A.J., Christensen, N.D., White, D.C., Wohl, E., Morrison, R.R., 2025. Trajectories of river-floodplain morphology and hydraulics following compounding wildfire-flood disturbances. Earth Surf. Process. Landf. 50 (5), e70057. https://doi.org/10.1002/esp.70057.
Hauer, F.R., Locke, H., Dreitz, V.J., Hebblewhite, M., Lowe, W.H., Muhlfeld, C.C., Nelson, C.R., Proctor, M.F., Rood, S.B., 2016. Gravel-bed river floodplains are the ecological nexus of glaciated mountain landscapes. Sci. Adv. 2, e1600026. https://doi.org/10.1126/sciadv.1600026.
Helton, A.M., Poole, G.C., Payn, R.A., Izurieta, C., Stanford, J.A., 2014. Relative influences of the river channel, floodplain surface, and alluvial aquifer on simulated hydrologic residence time in a montane river floodplain. Geomorphology 205, 17–26. https://doi.org/10.1016/j.geomorph.2012.01.004.
Hiemstra, K.S., Van Vuren, S., Vinke, F.S.R., Jorissen, R.E., Kok, M., 2020. Assessment of the functional performance of lowland river systems subjected to climate change and large-scale morphological trends. Int. J. River Basin Manag. 20, 45–56. https://doi.org/10.1080/15715124.2020.1790580.
Hortobagyi, B., Petit, S., Marteau, B., Melun, G., Piegay, H., 2024. A high-resolution inter-annual framework for exploring hydrological drivers of large wood dynamics. River Res. Appl. 40, 958–975. https://doi.org/10.1002/rra.4242.
Hurvich, C.M., Tsai, C.-L., 1989. Regression and time series model selection in small samples. Biometrika 76 (2), 297–307. https://doi.org/10.1093/biomet/76.2.297.
Iskin, E.P., Wohl, E., 2023. Quantifying floodplain heterogeneity with field observation, remote sensing, and landscape ecology: Methods and metrics. River Res. Appl. 39 (5), 911–929. https://doi.org/10.1002/rra.4109.
Jarrett, R.D., 1990. Paleohydrologic techniques used to define the spatial occurrence of floods. Geomorphology 3 (2), 181–195. https://doi.org/10.1016/0169-555X(90)90044-Q.
Kean, J.K., Schmitt, Robert G., Rengers, Francis K., Jason, W., 2022, February 24. Cameron peak fire: Flooding and debris flows. ArcGIS StoryMaps https://storymaps.arcgis.com/stories/af3cd28cad6040e9a3a3d608f58292a7.
Kellerhals, R., Church, M., 1989. The morphology of large rivers: characterisation and management. Canadian Special Publications of Fisheries and Aquatic Science 106, 31–48.
Kemp, J.L., Harper, D.M., Crosa, G.A., 1999. Use of 'functional habitats' to link ecology with morphology and hydrology in river rehabilitation. Aquat. Conserv. Mar. Freshwat. Ecosyst. 9, 159–178. https://doi.org/10.1002/(SICI)1099-0755(199901/02)9:1%3C159::AID-AQC319%3E3.0.CO;2-M.
Kornse, Z., Wohl, E., 2020. Assessing restoration potential for beaver (castor canadensis) in the semiarid foothills of the Southern Rockies, USA. River Res. Appl. 36 (9), 1932–1943. https://doi.org/10.1002/rra.3719.
Kostelnik, J., Schmitt, R.G., Rengers, F.K., Kean, J.W., 2022. Cameron Peak Fire: Flooding and Debris Flows [Story Map]. https://landslides.usgs.gov/storymap/cameronpeak/.
Lane, S.N., 2017. Natural flood management. WIREs Water 4 (3), e1211. https://doi.org/10.1002/wat2.1211.
Langhans, S.D., Richard, U., Rueegg, J., Uehlinger, U., Edwards, P., Doering, M., Tockner, K., 2013. Environmental heterogeneity affects input, storage, and transformation of coarse particulate organic matter in a floodplain mosaic. Aquat. Sci. 75, 335–348. https://doi.org/10.1007/s00027-012-0277-0.
Larsen, A., Larsen, J.R., Lane, S.N., 2021. Dam builders and their works: Beaver influences on the structure and function of river corridor hydrology, geomorphology, biogeochemistry and ecosystems. Earth Sci. Rev. 218, 103623. https://doi.org/10.1016/j.earscirev.2021.103623.
Lininger, K.B., Latrubesse, E.M., 2016. Flooding hydrology and peak discharge attenuation along the middle Araguaia River in Central Brazil. Catena 143, 90–101. https://doi.org/10.1016/j.catena.2016.03.043.
Livers, B., Wohl, E., 2015. An evaluation of stream characteristics in glacial versus fluvial process domains in the Colorado Front Range. Geomorphology 231, 72–82. https://doi.org/10.1016/j.geomorph.2014.12.003.
Livers, B., Wohl, E., 2016. Sources and interpretation of channel complexity in forested subalpine streams of the Southern Rocky Mountains. Water Resour. Res. 52 (5), 3910–3929. https://doi.org/10.1002/2015WR018306.
Livers, B., Lininger, K.B., Kramer, N., Sendrowski, A., 2020. Porosity problems: comparing and reviewing methods for estimating porosity and volume of wood jams in the field. Earth Surf. Process. Landf. 45 (13), 3336–3353. https://doi.org/10.1002/esp.4969.
Madole, R.F., 1976. Glacial geology of the Front Range, Colorado. In: Quaternary Stratigraphy of North America. Dowden Hutchinson and Ross, Stroudsburg PA, pp. 297–318.
Manners, R.B., Doyle, M.W., Small, M.J., 2007. Structure and hydraulics of natural woody debris jams. Water Resour. Res. 43 (6), 2006WR004910. https://doi.org/10.1029/2006WR004910.
Marshall, A., Wohl, E., Iskin, E., Zeller, L., 2024. Interactions of logjams, channel dynamics, and geomorphic heterogeneity within a river corridor. Water Resour. Res. 60, e2023WR036512. https://doi.org/10.1029/2023WR036512.
McFeeters, S.K., 1996. The use of the Normalized Difference Water Index (Ndwi) in the delineation of open water features. Int. J. Remote Sens. 17 (7), 1425–1432. https://doi.org/10.1080/01431169608948714.
Meyer, S., McCormick, J.L., Copeland, T., Young, A., 2025. Ecological benefits and risks to native salmonids from beaver dam analogs. Front. Ecol. Evol. 13, 1683942. https://doi.org/10.3389/fevo.2025.1683942.
Miller, J.R., Germanoski, D., Lord, M.L., 2011. Geomorphic processes affecting meadow ecosystems. Geomorphol. Hydrology, Ecol. Gt. Basin Meadow Complexes—Implications Manag. Restor. 24. https://doi.org/10.2737/RMRS-GTR-258.
Moody, J.A., Martin, D.A., 2001. Initial hydrologic and geomorphic response following a wildfire in the Colorado front range. Earth Surf. Process. Landf. 26 (10), 1049–1070. https://doi.org/10.1002/esp.253.
Morrison, R.R., Jones, C.N., Lininger, K., Thoms, M.C., Wohl, E., 2024. Resilient floodplains in the Anthropocene. In: Thoms, M., Fuller, I. (Eds.), Resilience and Riverine Landscapes. Elsevier, pp. 41–68. https://doi.org/10.1016/B978-0-323-91716-2.00035-2.
Moyle, P.B., Mount, J.F., 2007. Homogenous rivers, homogenous fauna. Proc. Natl. Acad. Sci. 104, 5711–5712. https://doi.org/10.1073/pnas.0701457104.
Ockelford, A., Wohl, E., Ruiz-Villanueva, V., Comiti, F., Piégay, H., Darby, S., Parsons, D., Yochum, S.E., Wolstenholme, J., White, D., Uno, H., Triantafillou, S., Stroth, T., Smrdel, T., Scott, D.N., Scamardo, J.E., Rees, J., Rathburn, S., Morrison, R.R., Aarnink, J., 2024. Working with wood in rivers in the Western United States. River Res. Appl. 40 (8), 1626–1641. https://doi.org/10.1002/rra.4331.
Pavlowsky, R.T., Hess, J.W., Martin, D.J., Dogwiler, T., Bendix, J., 2023. Large wood loads in channels and on floodplains after a 500-year flood using UAV imagery in Mark Twain National Forest, Ozark Highlands. Missouri. Geomorphology 431, 108672. https://doi.org/10.1016/j.geomorph.2023.108672.

Pearce, C., Vidon, P., Lautz, L., Kelleher, C., Davis, J., 2021. Impact of beaver dam analogues on hydrology in a semi-arid floodplain. Hydrol. Process. 35 (7), e14275. https://doi.org/10.1002/hyp.14275.
Pederson, G.T., Betancourt, J.L., McCabe, G.J., 2013. Regional patterns and proximal causes of the recent snowpack decline in the Rocky Mountains, U.S. Geophys. Res. Lett. 40 (9), 1811–1816. https://doi.org/10.1002/grl.50424.
Peipoch, M., Brauns, M., Hauer, F.R., Weitere, M., Valett, H.M., 2015. Ecological simplification: human influences on riverscape complexity. BioScience 65, 1057–1065. https://doi.org/10.1093/biosci/biv120.
Pelletier, J.D., Orem, C.A., 2014. How do sediment yields from post-wildfire debris-laden flows depend on terrain slope, soil burn severity class, and drainage basin area? Insights from airborne-LiDAR change detection. Earth Surf. Process. Landf. 39 (13), 1822–1832. https://doi.org/10.1002/esp.3570.
Pollock, M.M., Beechie, T.J., Jordan, C.E., 2007. Geomorphic changes upstream of beaver dams in Bridge Creek, an incised stream channel in the interior Columbia River basin, eastern Oregon. Earth Surf. Process. Landf. 32, 1174–1185. https://doi.org/10.1002/esp.1553.
Polvi, E.E., Wohl, E.E., Merritt, D.M., 2011. Geomorphic and process domain controls on riparian zones in the Colorado Front Range. Geomorphology 125, 504–516. https://doi.org/10.1016/j.geomorph.2010.10.012.
Polvi, L.E., Wohl, E., 2012. The beaver meadow complex revisited – the role of beavers in post-glacial floodplain development. Earth Surf. Process. Landf. 37 (3), 332–346. https://doi.org/10.1002/esp.2261.
Polvi, L.E., Wohl, E., 2013. Biotic drivers of stream planform. BioScience 63 (6), 439–452. https://doi.org/10.1525/bio.2013.63.6.6.
Powers, P.D., Helstab, M., Niezgoda, S.L., 2019. A process-based approach to restoring depositional river valleys to stage 0, an anastomosing channel network. River Res. Appl. 35 (1), 3–13. https://doi.org/10.1002/rra.3378.
Pugh, B.E., Colley, M., Dugdale, S.J., Edwards, P., Flitcroft, R., Holz, A., Johnson, M., Mariani, M., Means-Brous, M., Meyer, K., Moffett, K.B., Renan, L., Schrodt, F., Thorne, C., Valman, S., Wijayratne, U., Field, R., 2022. A possible role for river restoration enhancing biodiversity through interaction with wildfire. Glob. Ecol. Biogeogr. 31 (10), 1990–2004. https://doi.org/10.1111/geb.13555.
Puttock, A., Graham, H.A., Ashe, J., Luscombe, D.J., Brazier, R.E., 2021. Beaver dams attenuate flow: a multi-site study. Hydrol. Process. 35 (2), e14017. https://doi.org/10.1002/hyp.14017.
Rakholia, S., Mehta, A., Suthar, B., 2020. Forest fire monitoring of Shoolpaneshwar Wildlife Sanctuary, Gujarat, India using geospatial techniques. Curr. Sci. 119 (12), 1974. https://doi.org/10.18520/cs/v119/i12/1974-1981.
Rinaldi, M., Surian, N., Comiti, F., Bussettini, M., 2013. A method for the assessment and analysis of the hydromorphological condition of Italian streams: the morphological quality index (MQI). Geomorphology 180-181, 96–108. https://doi.org/10.1016/j.geomorph.2012.09.009.
Rinaldi, M., Surian, N., Comiti, F., Bussettini, M., 2015. A methodological framework for hydromorphological assessment, analysis and monitoring (IDRAIM) aimed at promoting integrated river management. Geomorphology 251, 122–136. https://doi.org/10.1016/j.geomorph.2015.05.010.
Rood, S.B., Pan, J., Gill, K.M., Franks, C.G., Samuelson, G.M., Shepherd, A., 2008. Declining summer flows of Rocky Mountain rivers: changing seasonal hydrology and probable impacts on floodplain forests. J. Hydrol. 349 (3), 397–410. https://doi.org/10.1016/j.jhydrol.2007.11.012.
Ryan, S.E., Shobe, C.M., Rathburn, S.L., Dixon, M.K., 2024. Suspended-sediment response to wildfire and a major post-fire flood on the Colorado Front Range. River Res. Appl. 40 (7), 1256–1272. https://doi.org/10.1002/rra.4286.
Schulz, E.Y., Morrison, R.R., Bailey, R.T., Raffae, M., Arnold, J.G., White, M.J., 2024. River corridor beads are important areas of floodplain-groundwater exchange within the Colorado River headwaters watershed. Hydrol. Process. 38, e15282. https://doi.org/10.1002/hyp.15282.
Schumm, S., Harvey, M., Watson, C., 1984. Incised Channels: Morphology, Dynamics and Control. Water Resources Publications, Littleton, Colorado.
Serra-Llobet, A., Jahnig, S.C., Geist, J., Kondolf, G.M., Damm, C., Scholz, M., Lund, J., Opperman, J.J., Yarnell, S.M., et al., 2022. Restoring rivers and floodplains for habitat and flood risk reduction: experiences in multi-benefit floodplain management from California and Germany. Front. Environ. Sci. 9, 778568. https://doi.org/10.3389/fenvs.2021.778568.
Shields, F.D., Smith, R.H., 1992. Effects of large woody debris on physical characteristics of a sand-bed river. Aquat. Conserv. Mar. Freshwat. Ecosyst. 2, 145–163. https://doi.org/10.1002/aqc.3270020203.
Smith, B., Clifford, N.J., Mant, J., 2014. The changing nature of river restoration. WIREs Water 1, 249–261. https://doi.org/10.1002/wat2.1021.
Solander, K.C., Bennett, K.E., Fleming, S.W., Gutzler, D.S., Hopkins, E.M., Middleton, R. S., 2018. Interactions between climate change and complex topography drive observed streamflow changes in the Colorado river basin. J. Hydrometeorol. 19 (10), 1637–1650. https://doi.org/10.1175/JHM-D-18-0012.1.
Spurgeon, J.J., Pegg, M.A., Parasiewicz, P., Rogers, J., 2018. Diversity of river fishes influenced by habitat heterogeneity across hydrogeomorphic divisions. River Res. Appl. 34 (7), 797–806. https://doi.org/10.1002/rra.3306.
Stanford, J.A., Ward, J.V., 1993. An ecosystem perspective of alluvial rivers: Connectivity and the hyporheic corridor. J. N. Am. Benthol. Soc. 12 (1), 48–60. https://doi.org/10.2307/1467685.
Stoffers, T., Buijse, A.D., Geerling, G.W., Jans, L.H., Schoor, M.M., Poos, J.J., Verreth, J. A.J., Nagelkerke, L.A.J., 2022. Freshwater fish biodiversity restoration in floodplain rivers requires connectivity and habitat heterogeneity at multiple spatial scales. Sci. Total Environ. 838, 156509. https://doi.org/10.1016/j.scitotenv.2022.156509.
Sutfin, N.A., Wohl, E., Fegel, T., Day, N., Lynch, L., 2021. Logjams and channel morphology influence sediment storage, transformation of organic matter, and carbon storage within mountain stream corridors. Water Resour. Res. 57 (5), e2020WR028046. https://doi.org/10.1029/2020WR028046.
Swayze, N., Choi, C.T.H., Knowlton, G., Klisauskaite, J., 2021. Colorado Front Range disasters: Understanding the impact of forest management on the Cameron Peak and Calwood fire. https://ntrs.nasa.gov/citations/20210014944.
Thomas, R.F., Kingsford, R.T., Lu, Y., Cox, S.J., Sims, N.C., Hunter, S.J., 2015. Mapping inundation in the heterogeneous floodplain wetlands of the Macquarie Marshes, using Landsat Thematic Mapper. J. Hydrol. 524, 194–213. https://doi.org/10.1016/j.jhydrol.2015.02.029.
Thoms, M., Fuller, I., 2023. Resilience and Riverine Landscapes. Elsevier, Amsterdam, The Netherlands.
Thoms, M.C., Delong, M.D., Flotemersch, J.E., Collins, S.E., 2017. Physical heterogeneity and aquatic community function in river networks: a case study from the Kanawha River basin, USA. Geomorphology 290, 277–287. https://doi.org/10.1016/j.geomorph.2017.02.027.
Thurman, E.M., Ferrer, I., Bowden, M., Mansfeldt, C., Fegel, T.S., Rhoades, C.C., Rosario-Ortiz, F., 2023. Occurrence of benzene polycarboxylic acids in ash and streamwater after the Cameron peak fire. ACS ESandT Water 3 (12), 3848–3857. https://doi.org/10.1021/acsestwater.3c00246.
Triantafillou, S., Wohl, E., 2024. Geomorphic characteristics influencing post-fire river response in mountain streams. Geomorphology 466, 109446. https://doi.org/10.1016/j.geomorph.2024.109446.
Tweto, Ogden, 1979. Geologic Map of Colorado. 1:500,000. US Geological Survey. https://ngmdb.usgs.gov/Prodesc/proddesc_68589.htm.
USDA Forest Service, 2020. In: USDA Forest Service, Geospatial Technology and Applications Center, BAER Imagery Support Program (Ed.), Soil Burn Severity Dataset for the CAMERON PEAK Fire Occurring on the Arapaho and Roosevelt National Forests/Pawnee National Grassland National Forest: USDS Forest Service Raster Digital Data. https://fsapps.nwcg.gov/afm/baer/download.php.
Van Looy, K., Tonkin, J.D., Floury, M., Leigh, C., Soininen, J., Larsen, S., Heino, J., Poff, N.L., Delong, M., et al., 2019. The three Rs of river ecosystem resilience: resources, recruitment, and refugia. River Res. Appl. 35, 107–120. https://doi.org/10.1002/rra.3396.
Veblen, Thomas, Donnegan, Joseph, 2006. Historical Range of Variability of Forest Vegetation of the National Forests of the Colorado Front Range. USDA Forest Service, Rocky Mountain Region and the Colorado Forest Restoration Institute, Fort Collins, p. 151.
Verdonschot, P.F.M., Verdonschot, R.C.M., 2023. The role of stream restoration in enhancing ecosystem services. Hydrobiologia 850, 2537–2562. https://doi.org/10.1007/s10750-022-04918-5.
Walling, D.E., He, Q., 1998. The spatial variability of overbank sedimentation on river floodplains. Geomorphology 24, 209–223. https://doi.org/10.1016/S0169-555X(98)00017-8.
Westbrook, C.J., Cooper, D.J., Baker, B.W., 2006. Beaver dams and overbank floods influence groundwater–surface water interactions of a Rocky Mountain riparian area. Water Resour. Res. 42 (6), 2005WR004560. https://doi.org/10.1029/2005WR004560.
Westerling, A.L., 2016. Increasing western US forest wildfire activity: Sensitivity to changes in the timing of spring. Philos. Trans. R. Soc. B 371 (1696), 20150178. https://doi.org/10.1098/rstb.2015.0178.
Wilkinson, M.E., Addy, S., Quinn, P.F., Stutter, M., 2019. Natural flood management: small-scale progress and larger-scale challenges. Scott. Geogr. J. 135, 23–32. https://doi.org/10.1080/14702541.2019.1610571.
Wohl, E., 2016. Spatial heterogeneity as a component of river geomorphic complexity. Prog. Phys. Geogr. 40, 598–615. https://doi.org/10.1177/0309133316658615.
Wohl, E., 2021a. An integrative conceptualization of floodplain storage. Rev. Geophys. 59, e2020RG000724. https://doi.org/10.1029/2020RG000724.
Wohl, E., 2021b. Legacy effects of loss of beavers in the continental United States. Environ. Res. Lett. 16 (2), 025010. https://doi.org/10.1088/1748-9326/abd34e.
Wohl, E., Iskin, E.P., 2022. The transience of channel-spanning logjams in mountain streams. Water Resour. Res. 58 (5), e2021WR031556. https://doi.org/10.1029/2021WR031556.
Wohl, E., Scott, D.N., 2017. Wood and sediment storage and dynamics in river corridors. Earth Surf. Process. Landf. 42, 5–23. https://doi.org/10.1002/esp.3909.
Wohl, E., Kuzma, J.N., Brown, N.E., 2004. Reach-scale channel geometry of a mountain river. Earth Surf. Process. Landf. 29 (8), 969–981. https://doi.org/10.1002/esp.1078.
Wohl, E., Dwire, K., Sutfin, N., Polvi, L., Bazan, R., 2012. Mechanisms of carbon storage in mountainous headwater rivers. Nat. Commun. 3 (1), 1263. https://doi.org/10.1038/ncomms2274.
Wohl, E., Lininger, K.B., Scott, D.N., 2018. River beads as a conceptual framework for building carbon storage and resilience to extreme climate events into river management. Biogeochemistry 141 (3), 365–383. https://doi.org/10.1007/s10533-017-0397-7.
Wohl, E., Marshall, A.E., Scamardo, J., White, D., Morrison, R.R., 2022. Biogeomorphic influences on river corridor resilience to wildfire disturbances in a mountain stream of the Southern Rockies, USA. Sci. Total Environ. 820, 153321. https://doi.org/10.1016/j.scitotenv.2022.153321.
Wohl, E., Fryirs, K., Grabowski, R.C., Morrison, R.R., Sear, D., 2024a. Enhancing the natural absorbing capacity of rivers to restore their resilience. BioScience 74, 782–796. https://doi.org/10.1093/biosci/biae090.
Wohl, E., Rathburn, S., Dunn, S., Iskin, E., Katz, A., Marshall, A., Means-Brous, M., Scamardo, J., Triantafillou, S., Uno, H., 2024b. Geomorphic context in process-based river restoration. River Res. Appl. 40, 322–340. https://doi.org/10.1002/rra.4236.

Wohl, E., Scamardo, J.E., Morrison, R.R., 2025a. James Buttle Review: Bed, banks and beyond: River flood dynamics. Hydrol. Process. 39, e70131. https://doi.org/10.1002/hyp.70131.

Wohl, E., Cenderelli, D.A., Dwire, K.A., Ryan-Burkett, S.E., Young, M.K., Fausch, K.D., 2010. Large in-stream wood studies: A call for common metrics. Earth Surf. Process. Landf. 35 (5), 618–625. https://doi.org/10.1002/esp.1966.

Wohl, E., Clark, M., Li, L., Tetzlaff, D., Soulsby, C., 2025b. Knots in the strings: do small-scale river features shape catchment-scale fluxes? WIREs Water 12, e70036. https://doi.org/10.1002/wat2.70036.

Wolf, E.C., Cooper, D.J., Hobbs, N.T., 2007. Hydrologic regime and herbivory stabilize an alternative state in Yellowstone National Park. Ecol. Appl. 17 (6), 1572–1587. https://doi.org/10.1890/06-2042.1.

Wright, J.P., Jones, C.G., Flecker, A.S., 2002. An ecosystem engineer, the beaver, increases species richness at the landscape scale. Oecologia 132 (1), 96–101. https://doi.org/10.1007/s00442-002-0929-1.

Wyzga, B., Zawiejska, J., 2005. Wood storage in a wide mountain river: case study of the Czarny Dunajec, Polish Carpathians. Earth Surf. Process. Landf. 30, 1475–1494. https://doi.org/10.1002/esp.1204.

Zanewich, K.P., Rood, S.B., 2025. Regional differences in high elevation snowpack decline along the north American Rocky Mountains. Hydrol. Process. 39 (5), e70153. https://doi.org/10.1002/hyp.70153.